Monte Carlo simulations and radiation transport in medical physics

N. Chofor and B. Poppe

WG Medical Radiation Physics, Carl von Ossietzky University Oldenburg, Germany
Pius-Hospital, Clinic of Radiotherapy and Oncology, Georgstr 12, Oldenburg, Germany

Workshop on Monte Carlo Methods in Natural Sciences, in Engineering and in Economics

19-21 February 2013, DESY, Hamburg

Overview:

A Why Monte Carlo in radiation physics?

I Radiation Physics in Medicine

II Linear electron accelerators (linacs)

III Dose „Imaging“

B The EGS code system:

I Photon and Electron transport logic

II Efficiency enhancement tools (Variance reduction)

III Examples: Research applications and some commercialized systems

Oldenburg

Stadt der Wissenschaft 2009
Übermorgenstadt
OLDENBURG

- located approx. 150 km west of Hamburg and about 45 km west of Bremen.
- approx. 150.000 inhabitants

- **Oldenburg**: Low German word meaning „Old castle"
- Establishment of first castle not known, but from 12th century Oldenburg became the official residence of Saxon nobles (Counts of Oldenburg)
- cultural and commercial center of North-West Germany

- **Carl von Ossietzky University** was founded in 1973 (today approx. 13% off all citizens are students, 40% of all student members of DGMP studying in Oldenburg)

ems
european medical school
oldenburg-groningen

- **European Medical School Oldenburg-Groningen** was founded as new faculty of the University 2012, First Bi-Lateral Medical School in Europe

Medical Physics in Oldenburg

School of Medicine and Health Sciences

↓

Department of Medical Physics and Acoustics

- 8 full time professorships in different areas

↓

Medical Radiation Physics

Prof. Dr. Björn Poppe

Prof. Dr. emer. Dietrich Harder

Dr. phil. Antje Ruehmann

Dr. rer. nat. Ndimofor Chofor

Dr. rer. nat. Hui Khee Looe

+ approx. 20 (Physicicst, PhD and Grad. Students)

A Why Monte Carlo methods in radiation physics?

- To complement experimental results as well as other analytic methods
- Additional tool for assessing basic physical quantities either difficult or impractically measurable
- In radiation physics used to circumvent the use of the transport equation
- Provide solutions for complex events during radiation transport processes
- Guides the design and improvement of radiation detecting devices and methods, thereby broadening the scope of understanding for research and clinical processes
- In the domain of radiotherapy, Monte Carlo applications aim at optimizing the destruction of cancer cells while sparing normal healthy tissues to the benefit of the patient
- Guidance for radiation protection requirements

A Why Monte Carlo methods in radiation physics?
I Radiotherapy basics and radiation physics in medicine

- Cancer second most commom cause for death in Germany (25%)
  (500.000 new cancer cases/year)

- 50% of all patients receive a radiotherapy

- Use of ionising radiation to damage tumor cells (unfortunately also healthy tissue is damaged

- Major used radiation types
    - **Photons and Electrons (6MV-27MV)**
    - Protons and ions...(approx. 250MeV/u for p, 120-500MeV/u in ion therapy

- Repair mechanisms better in normal tissue

- Fractionated irradiation to allow tissue repair

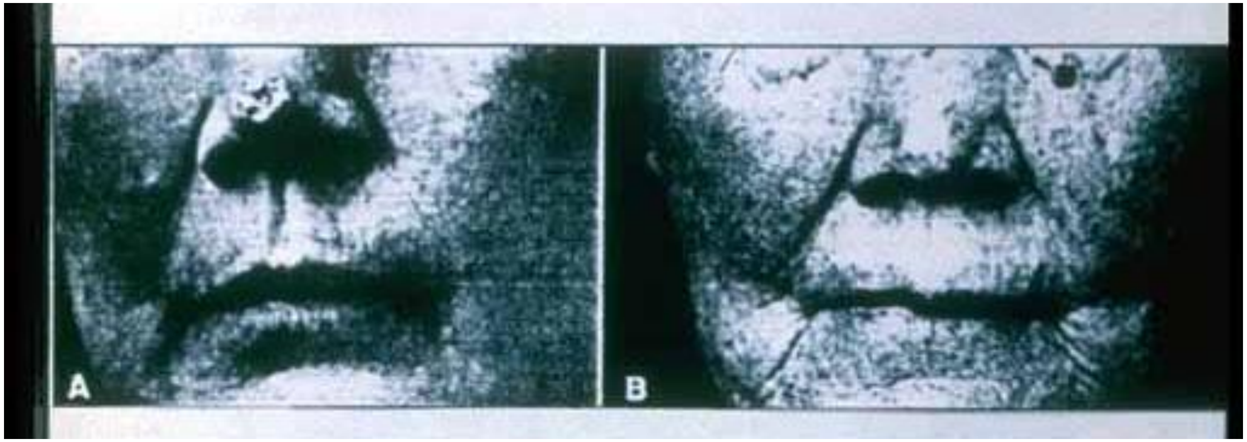

Fig. 1: One of the earliest radiotherapy applications: skin cancer ,100 fractions in 30 months. Foto left from 1899 (!!). Dose unknown!

First dose unit: Skin Erythema Dose

„The minimal dose of radiation required to cause perceptible reddening of the skin" (today 6-8Gy)

Ewing (1934):

„All one could really do was to place the patient under the machine and hope for the best"

Dose – The scalpel in „Radiotherapy“

Absorbed Dose: Gy = J/kg

$$D = \lim_{\Delta m \to 0} \frac{\Delta E}{\Delta m}$$

Total dose top tumor 50-80Gy in 1.8 - 2Gy/fraction

Tolerances Organs at Risk 5 - 54 Gy (5% risk in 5 years)

<u>Strategy in modern radiotherapy</u>

Optimal sparing of healthy organs

- Increase tumor doses with same side reaction probability
- Longer survival with better quality of life

A Why Monte Carlo methods in radiation physics?
II Linear electron accelerators (linacs)

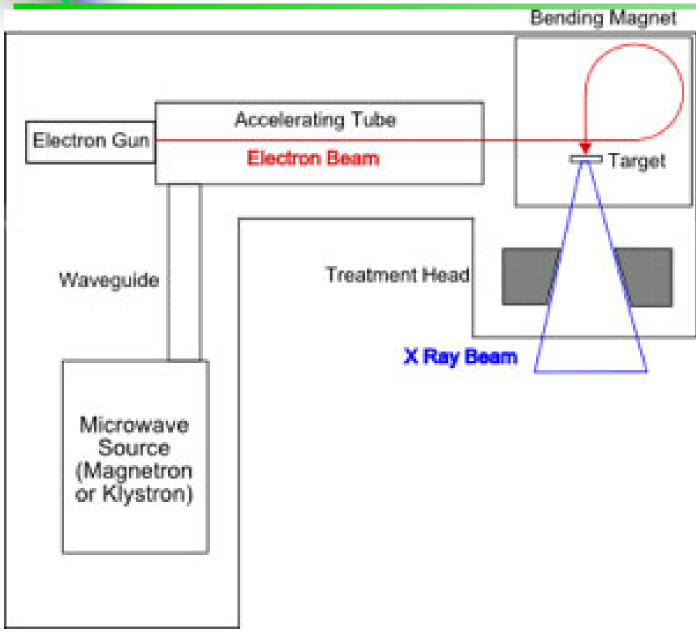

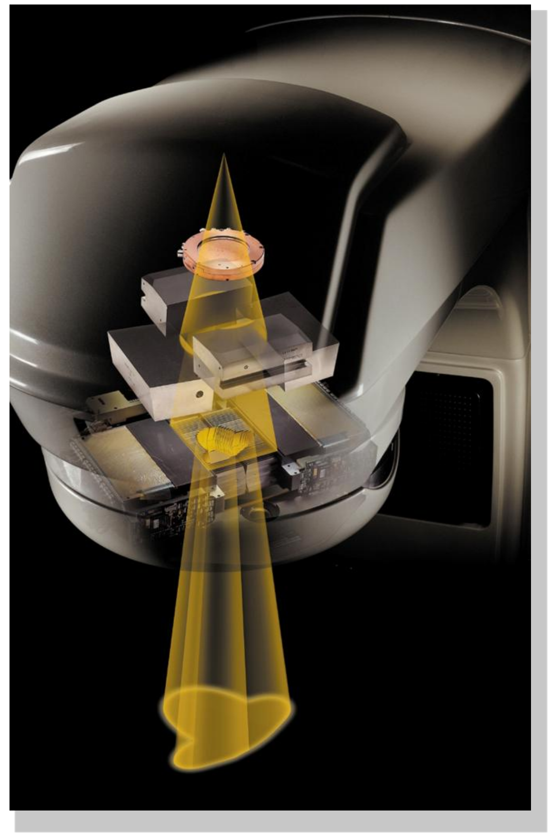

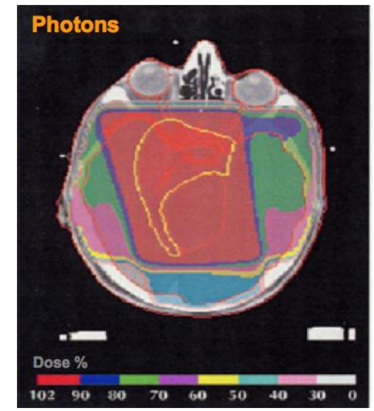

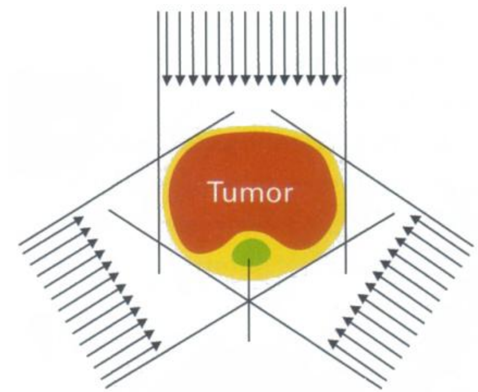

Fig. 2: Illustration of radiotherapy with medical linear electron accelerators. Gantry rotates: Tumor can be taken into "cross-fire". Leads to a reduction of dose outside tumor.

A Why Monte Carlo methods in radiation physics?
II Linear electron accelerators (linacs)

Dose Patterns:
Intensity Modulated Radiotherapy (**IMRT)**

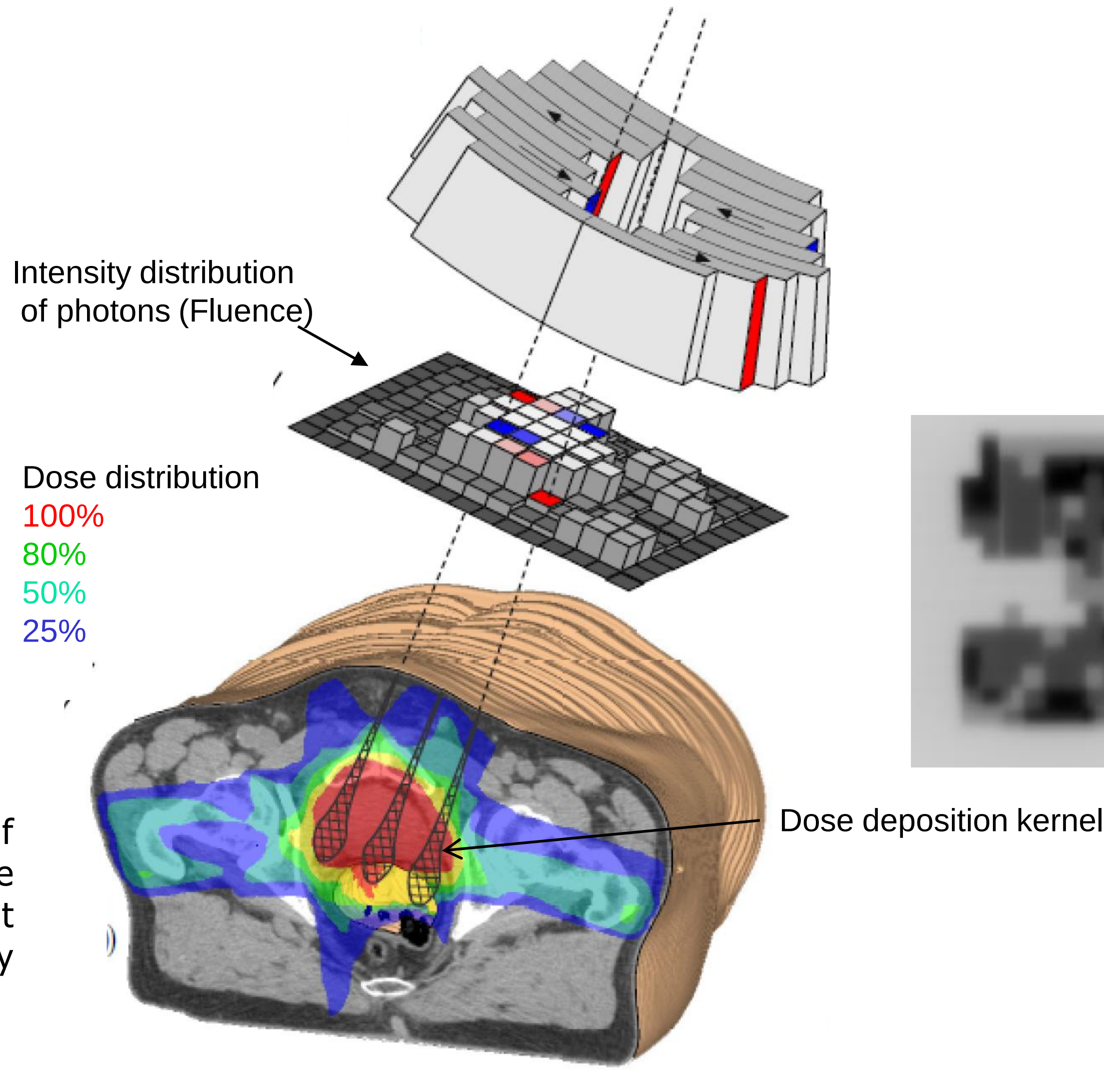

Fig. 3: The advent of multileaf collimators (MLCs), IMRT has become a dose delivery technique aimed at conforming the radiation intensity distribution to the shape of the tumor.

A Why Monte Carlo methods in radiation physics?
II Linear electron accelerators (linacs)

Other techniques

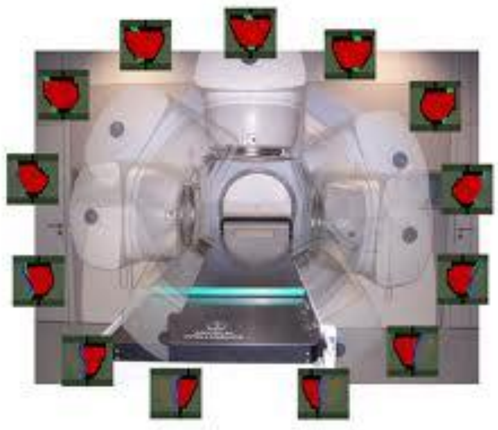

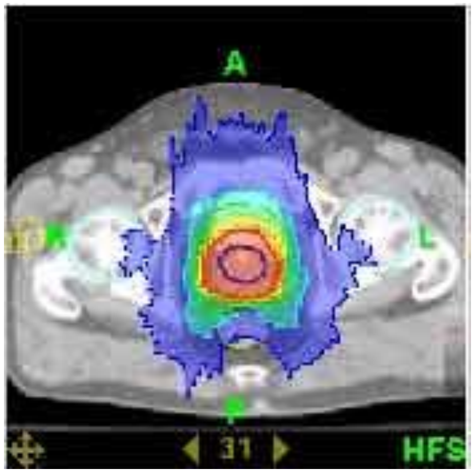

Arc-Therapy

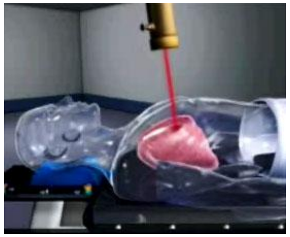

CyberKnife

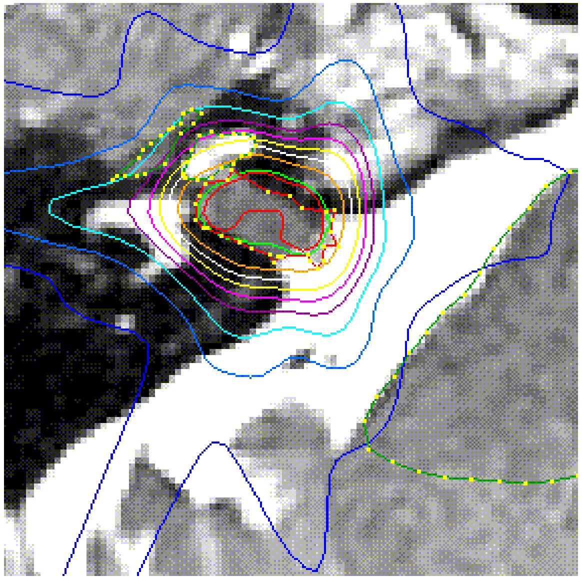

Fig. 4: Solving the inverse problem of dose patterns lead to a boom in new dose delivery techniques

A Why Monte Carlo methods in radiation physics?
II Linear electron accelerators (linacs)

Other techniques

Intra-operative radiotherapy (IORT)

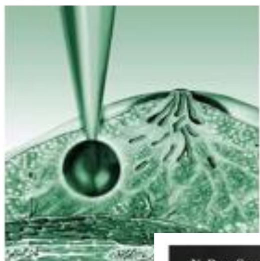

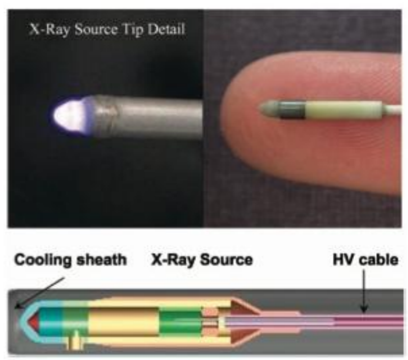

Brachytherapy

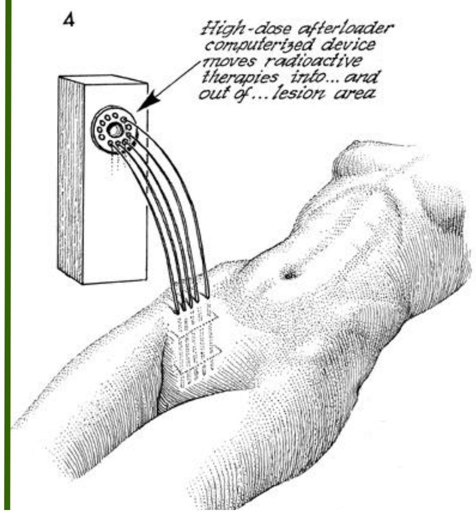

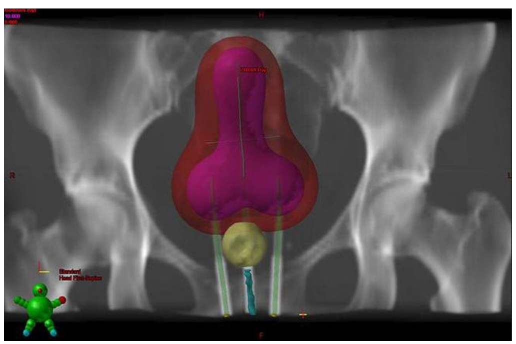

Fig. 5: Also available are classical treatment techniques based on placing the radiation source in close vicinity of tumor ("brachy" therapy).

A Why Monte Carlo methods in radiation physics?
II Dose „Imaging“

Modelling

Monte Carlo
and Analytical Methods

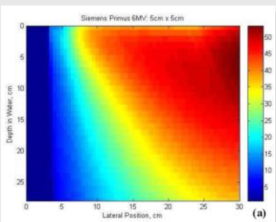

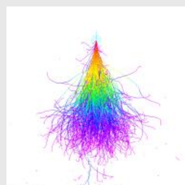

$$D(x)=\frac{1}{2arctg(a/\lambda)}\left\{\frac{c\lambda}{2D}\ln\frac{1+\left(\frac{a}{\lambda}-\frac{x}{\lambda}\right)^{2}}{1+\left(\frac{a}{\lambda}+\frac{x}{\lambda}\right)^{2}}+\left(1+\frac{C\lambda}{D}\frac{x}{\lambda}\right)\left[arctg\left(\frac{a}{\lambda}+\frac{x}{\lambda}\right)+arctg\left(\frac{a}{\lambda}-\frac{x}{\lambda}\right)\right]\right\}$$

Measurement

Detector Development

in Cooperation
with PTW
(„Octavius Detector Arrays Family“)

Clinical Transfer

DIN NA 080 Normenausschuss Radiologie (NAR)

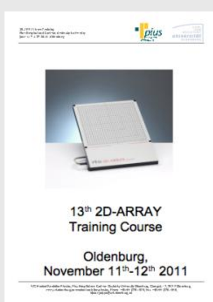
13th 2D-ARRAY
Training Course

Oldenburg,
November 11th-12th 2011


Independent dose and MU verification for IMRT patient specific quality assurance: Report of AAPM Task Group 219

Description of dose deposition and measurement process using signal theory

-Theoretical description of the spatial dose distribution (for predicting the dose distribution within the patient)

- Functioning principle: the dose deposition is described as

Integral of the convolution of the fluence distribution with an elementary dose deposition kernel

$$D(x,y,z) = \iiint \Phi(x',y',z') K(x-x', y-y', z-z') dV'$$

Φ : Fluence distribution of photons

K : Convolution kernel

Theoretical method: Monte Carlo kernels
Half-empirical methods: Analytic kernels

Dose deposition kernels

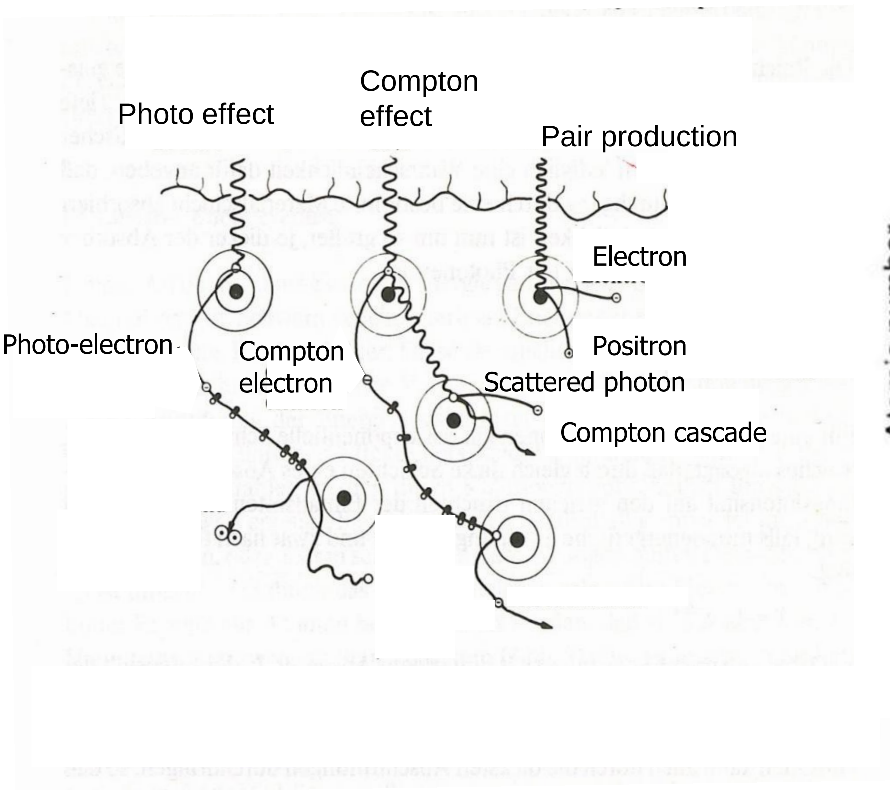

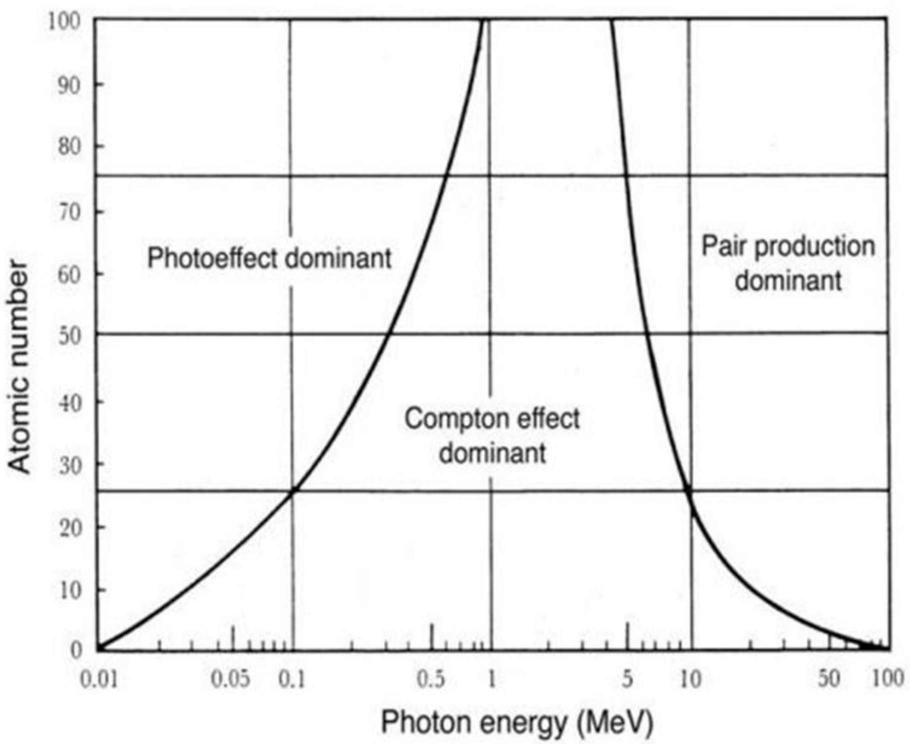

Fig. 6: Left: Basic interaction mechanisms following photon interaction with matter. Right: Regions of relative predominance of three main forms of photon interaction with matter. Shows interaction mechanisms relevant in radiotherapy and radiology applications.

A Why Monte Carlo methods in radiation physics? II Dose „Imaging“

GOAL: to obtain realistic dose distributions, as are expected via analogue computation, but in an economical way

Mohan and Chui (1987) first dose deposition kernels (MC Simulationen)

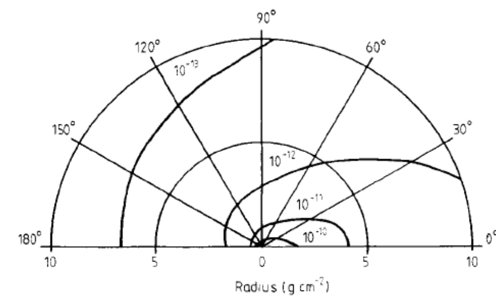

Figure 6. Total energy deposition kernel in isoline format for 1.25 MeV photons. The total energy deposition kernel is the sum of all the energy deposition kernel components. The units are cGy MeV^{-1} photon^{-1}.

Ahnesjö (1990s), popular analytic description

$$K_{PB}(r,z) = \frac{A_z e^{-a_z r}}{r} + \frac{B_z e^{-b_z r}}{r}$$

Ulmer (1997), 3 Gauß functions, Gauß plus Yukawa

$$D(r,z) = I(z)\left[a_1 \frac{e^{-r^2/\sigma^2(z)}}{\pi\sigma^2(z)} + a_2 \varepsilon(z) \frac{e^{-\varepsilon(z) r}}{2\pi r}\right]$$

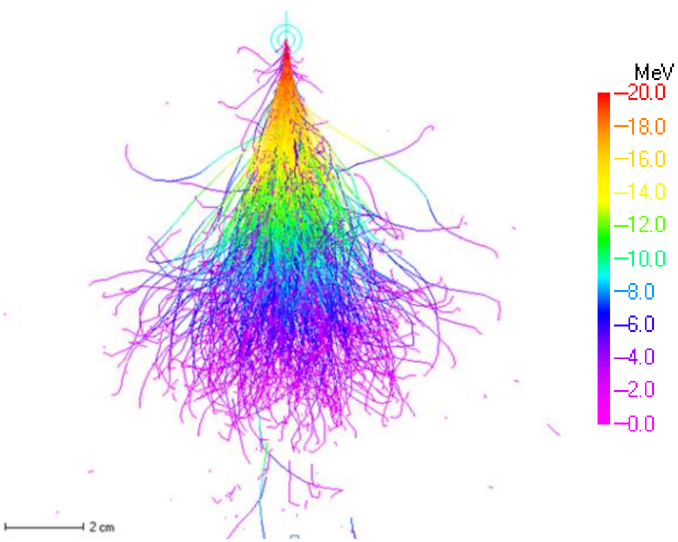

Fig. 7: Complete tracking of all basic interaction mechanisms would result in the correct dose distribution. Dose deposition kernels aim at simplifying these events for daily clinical applications, serving as the work engine of computer-based treatment planning systems.

Dose deposition kernels: small fields

$$D(x) = \Phi(x) * K(x)$$

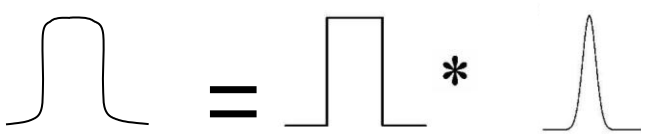

Dose profile = Fluence profile at the level of the beam collimating system * Effects of the system (Radiation generation and transport)

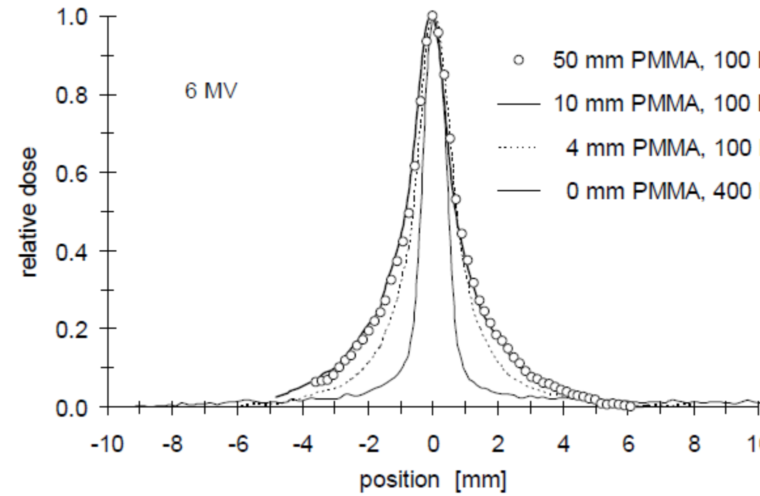

Fig. 8: Expected form of K(x), measured with a slit beam

Ansatz:
Numerical deconvolution, considering an ideal fluence distribution and analysis of the fluence in Fourier space

Following the folding law: $$FT[K(x)] = FT[D(x)] : FT[\Phi(x)]$$

A Why Monte Carlo methods in radiation physics?
II General purpose MC codes

- **ETRAN** (Berger and Seltzer, NIST, 1978)
- **MCNP5** (Los Alamos; 1990 – MCNP4)
- **EGS4** (Nelson, Hirayama and Rogers; SLAC 1985)
- **EGSnrc** (Kawrakow and Rogers; NRC 2003)
- **GEANT4** (Pia et al., CERN, 2005)
- **FLUKA** (Ferrari et al., CERN, 2005)
- **EGS5** (Hirayama et al., SLAC-KEK, 2005)
- **PENELOPE** (Salvat et al., UB, 1996-2005)

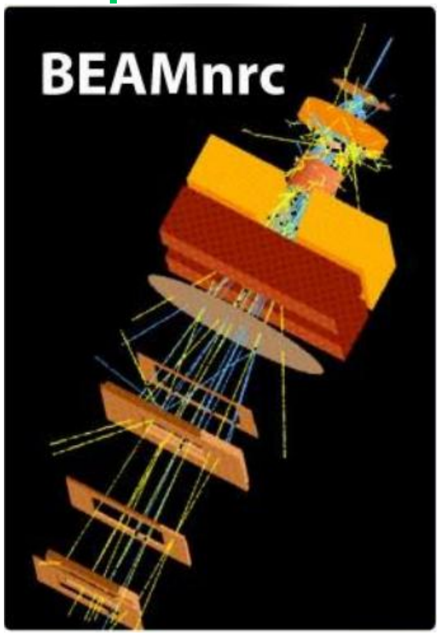

- *Full linear electron accelerator simulations*

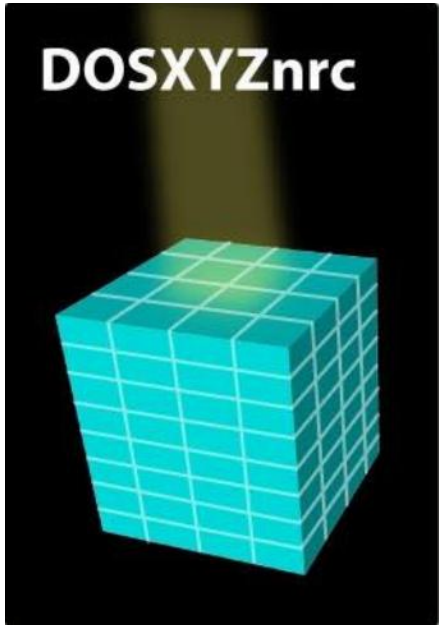

- *Dose computations within voxelized phantoms*

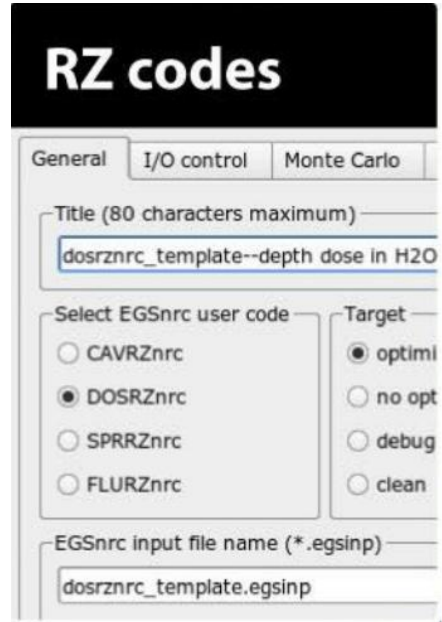

- *Computation within cylindrical geometries*

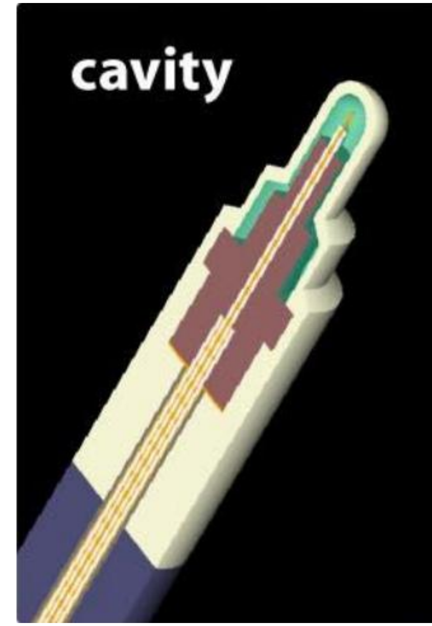

- *Simulation of exact radiation detector geometries*

Fig. 9: User codes for the EGSnrc system

A Why Monte Carlo methods in radiation physics?
II EGSnrc case study

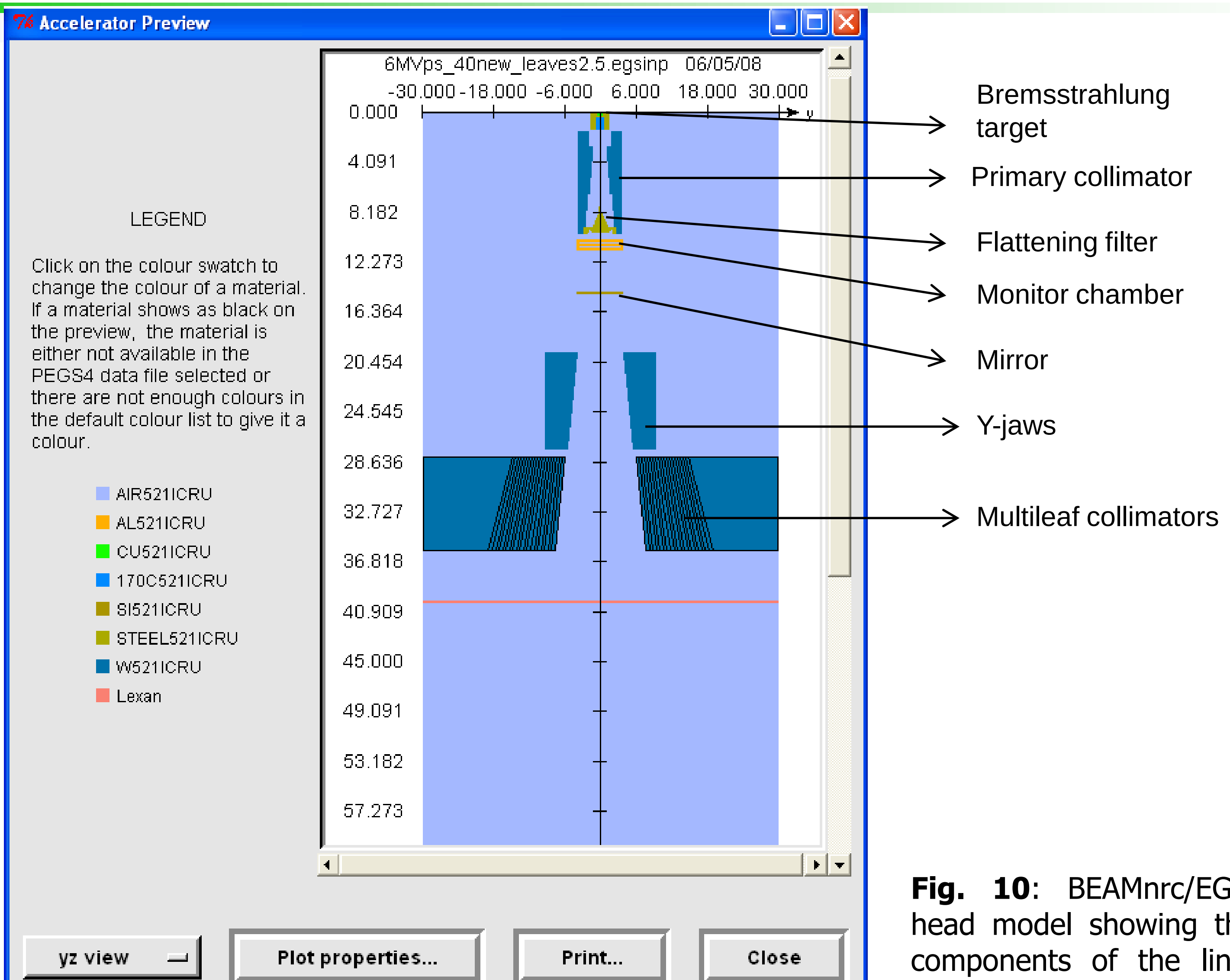

Fig. 10: BEAMnrc/EGSnrc: beam head model showing the simulated components of the linear electron accelerator head

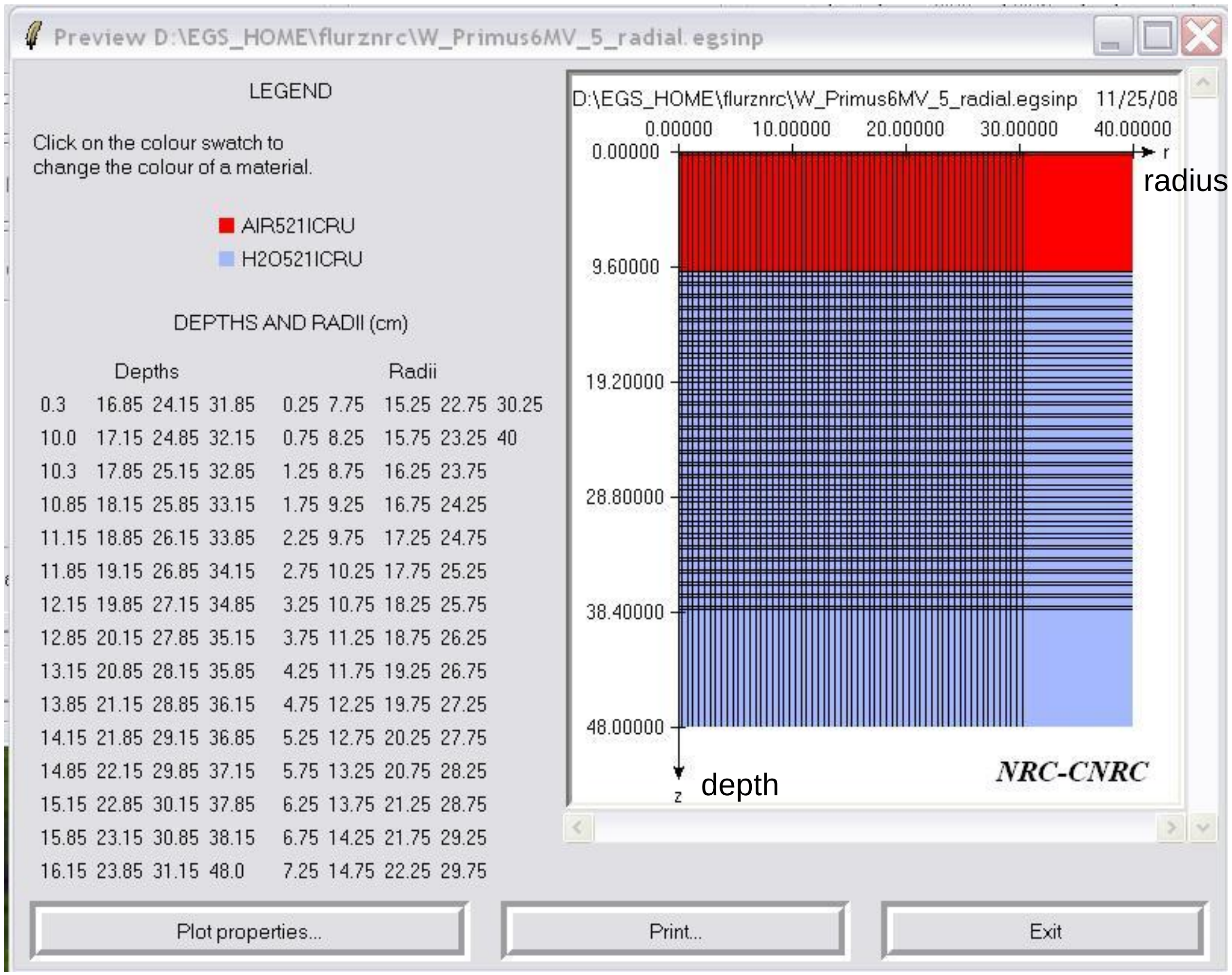

Fig. 11: FLURZnrc/EGSnrc: Scoring geometry for computing spectra within large water phantom, Z-R plane

B The EGS code system Structure

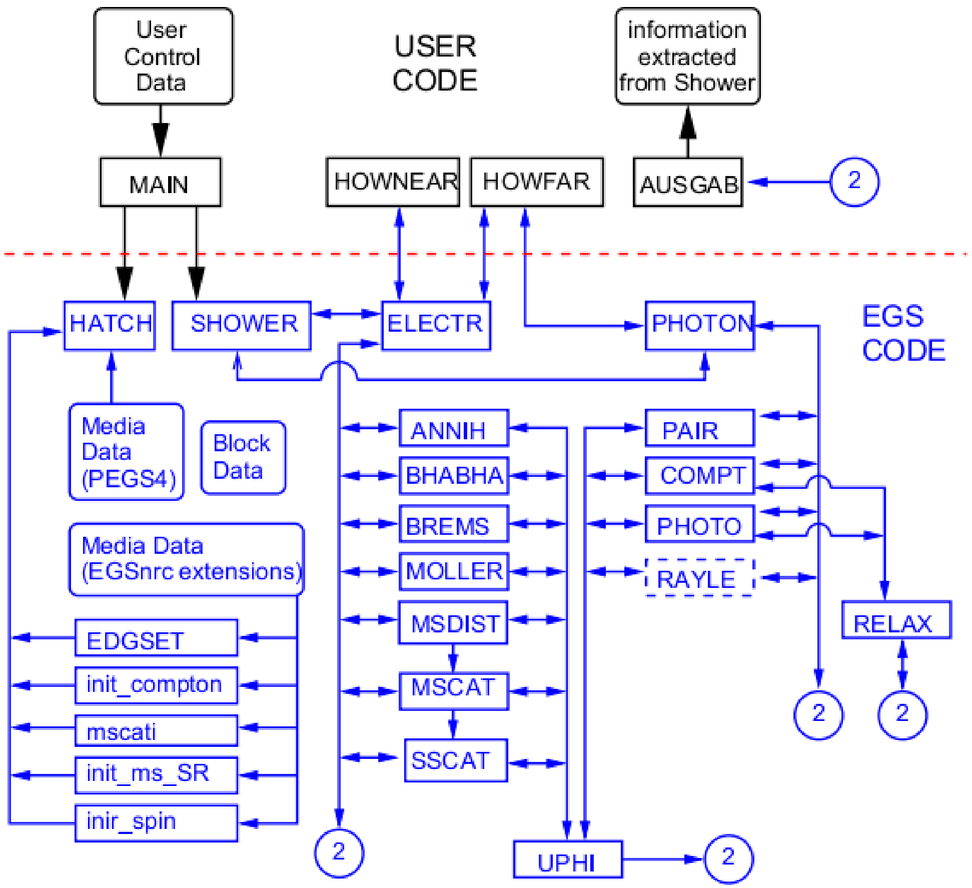

Fig. 12: Structure of the EGSnrc code system, showing the user area and the underlying code section.

- EGS4(Electron-Gamma-Shower), developed initially by Richard Ford and Ralph Nelson at SLAC
- EGSnrc, an extension of EGS4, adapted to medical applications via collaboration with the NRC
- User-friendly environment, to model geometry without altering the code
- HATCH: establish media data
- SHOWER: initiate cascade
- HOWNEAR + HOWFAR: geometry
- AUSGAB: score output and variance reduction control

B The EGS code system
Underlying physics

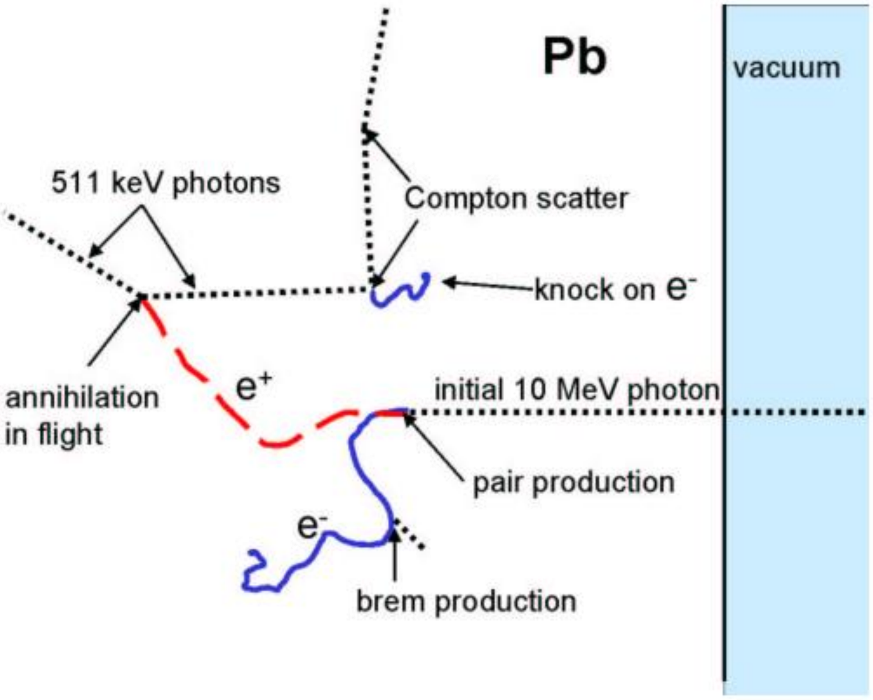

Fig. 13: Events following the incidence of a 10 MeV photon on a lead block from the right. A cascade of events follow .

- Photon interactions: 4 basic processes

(i) Energy transfer to electron/positron pair

(ii) Compton scatter (incoherent)

(iii) Photo-electric absorption

(iv) Rayleigh scatter (coherent)

- Electron interactions:

(i) Inelactic collisions with atomic electrons

(ii) Radiative loss (e.g. Bremsstrahlung and positron annihilation)

- Coupled electron and photon transport must be performed

I

Photon transport logic

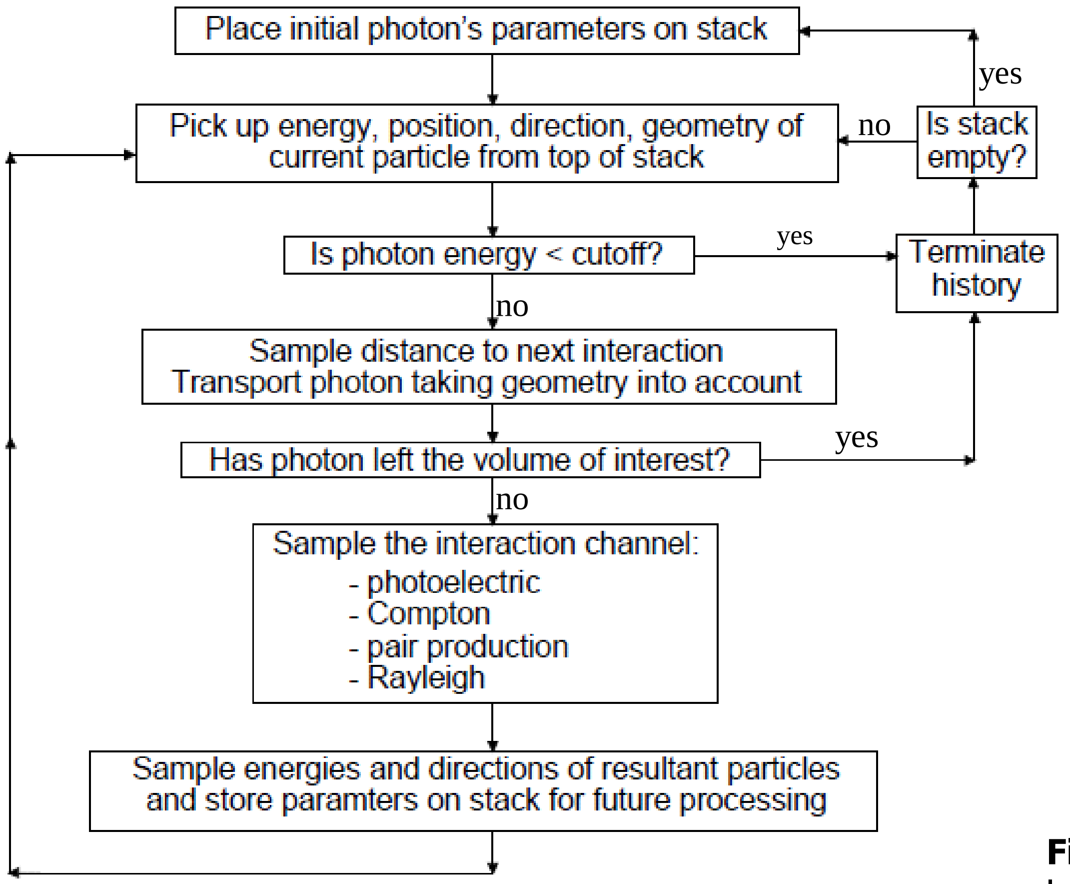

- Straight-forward
- **Class II** type (analogue) technique, following all interactions until particle falls below threshold energy or leaves geometry

Fig. 14: Flow chart of the photon transport logic in the EGSnrc Monte Carlo system.

B The EGSnrc system

I Electron transport logic

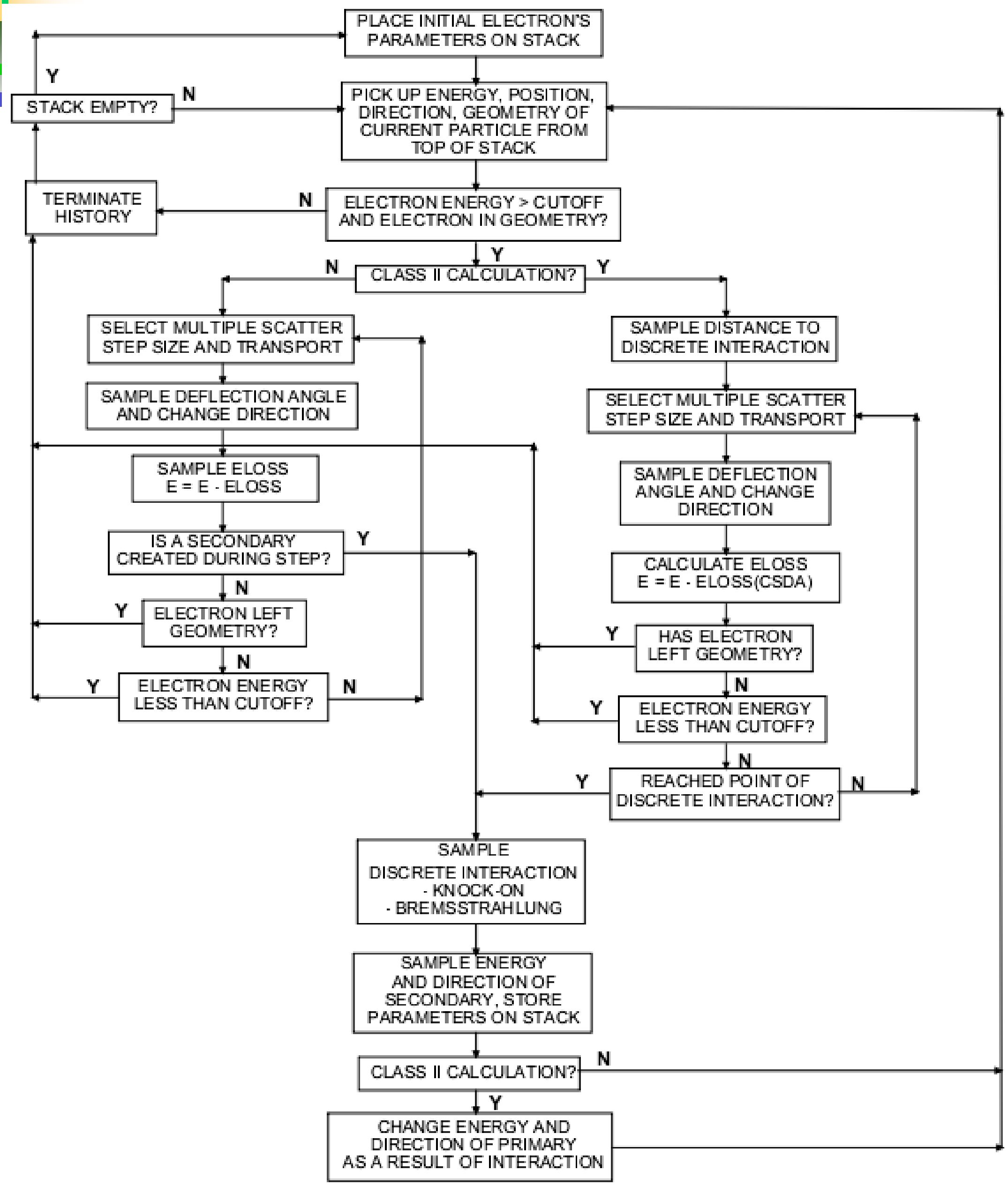

- Keep in mind the typically low energy loss of ca. 30 eV during electron and positron interactions with matter

- Millions of histories required for a Megavoltage incident beam

- Cumbersome !

- **Class I**: Solution is to group many small interactions into one step (Condensed History technique)

Fig. 15: Flow chart of the electron transport logic in the EGSnrc system.

Condensed History technique

- Condensed history technique describing the transport of electrons in MC techniques

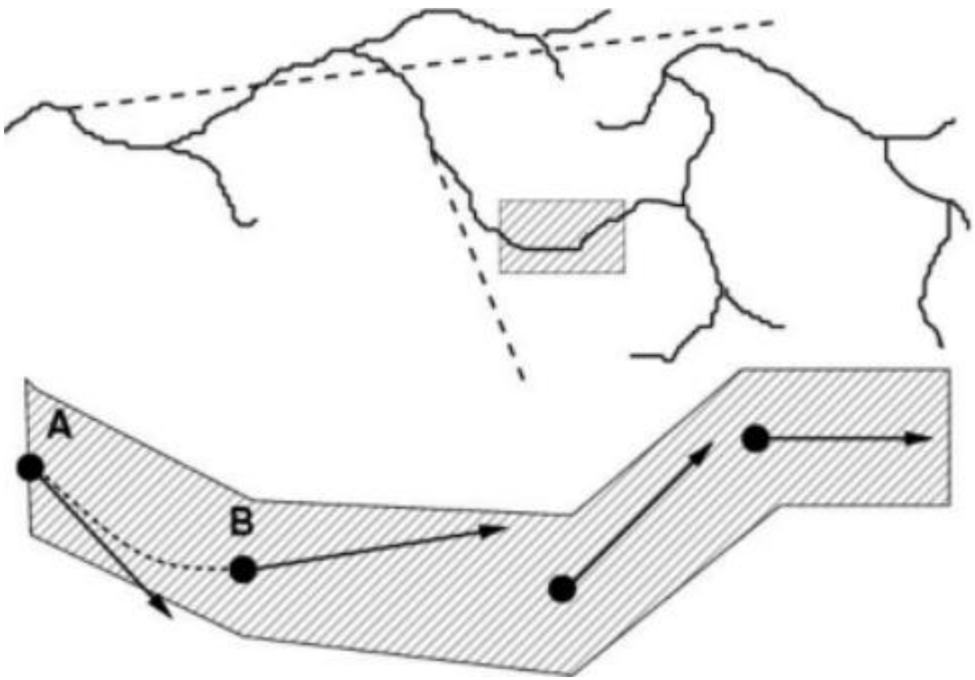

Fig. 16: Illustration of the condensed history technique used for electron transport logic.

III Efficiency enhancement tools

- Energy deposition and resulting distributions from treatment units could be obtained via (i) empirical or semi-empirical source models, (ii) compact representation of phase space (PS) data from full simulations and (iii) use of full phase space data

- Full PS data:

(i) Large amounts of data, i.e. up to a few gigabytes of data

(ii) Must be generated for each field setting

(iii) Limits the efficiency of fast MC applications, e.g. data retreiving over networks cumbersome

- **Goals**:

(i) Circumvent the intermediate storage of PS data

(ii) Avoid particle recycling (i.e. reusing particles in PS data)

- **Solution**:

(i) Use so-called **directional bremsstrahlung splitting** (DBS) during linac simulation (BEAMnrc)

(ii) Run phantom simulations (DOSXYZnrc), using the linac compiled as a shared source for input

(iii) Particles which would otherwise be stored in PS files in standard simulation are now stored in container array and are used in DOSXYZnrc

III Efficiency enhancement tools
- directional bremsstrahlung splitting (DBS) -

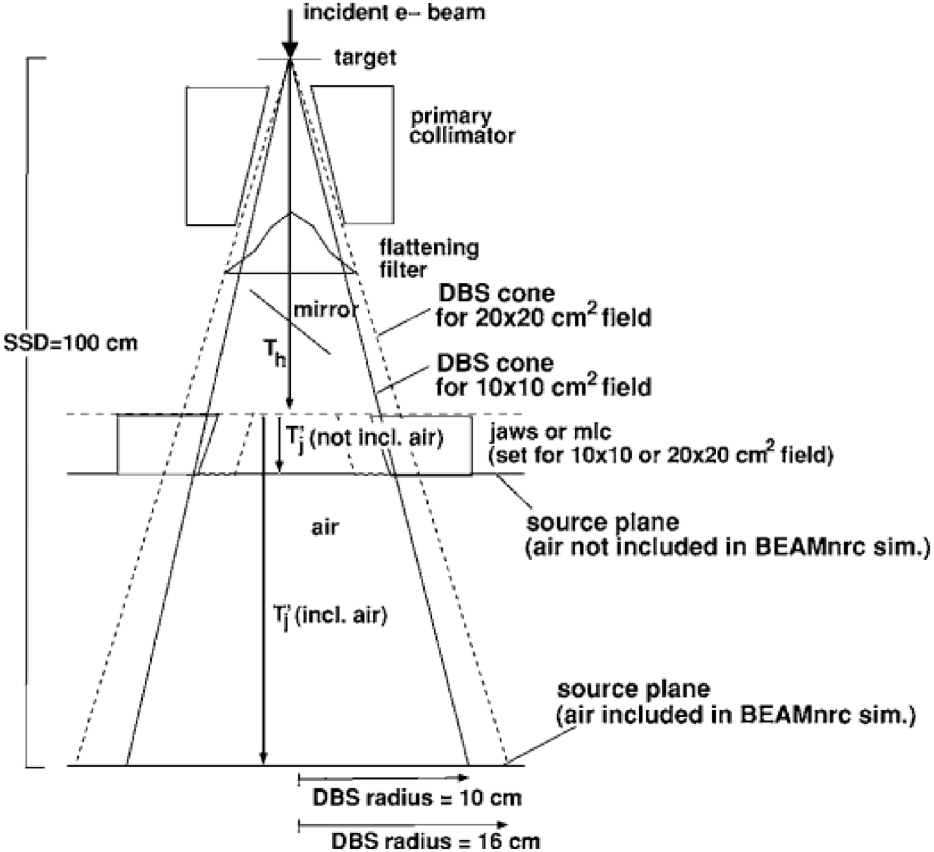

(a) BEAMnrc

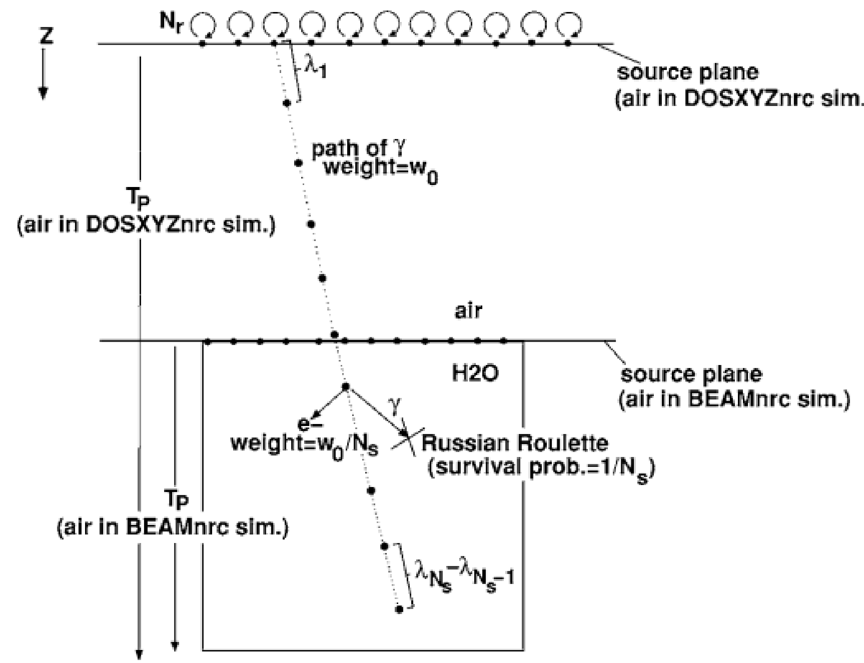

(b) DOSXYZnrc

Fig. 17: (a) Description of the parameters behind the DBS technique and (b) Illustration of the photon splitting technique to increase the sources of generated charged particles the Russian Roulette method to determine the fate of the photons generated during interactions.

III Efficiency enhancement tools
- directional bremsstrahlung splitting (DBS) -

- **Goal of DBS**: To improve the efficiency of charge particle generation without biasing the results

- **Method**:

(i) Photons of initial weight w_0 entering DOSXYZnrc are split *n-split* times (user-defined)
(ii) Each split photon assigned a statistical weight w_0 / *n-split*
(iii) Interaction sites of split photons distributed evenly along original photon path
(iv) Scattered photons resulting from interactions subject to Russian Roulette with survival probability 1 / *n-split*
(v) Charged particle retained with weight w_0 / *n-split*

- **Result**: Significantly improved efficiency compared to full phase space data reusage with particle splitting

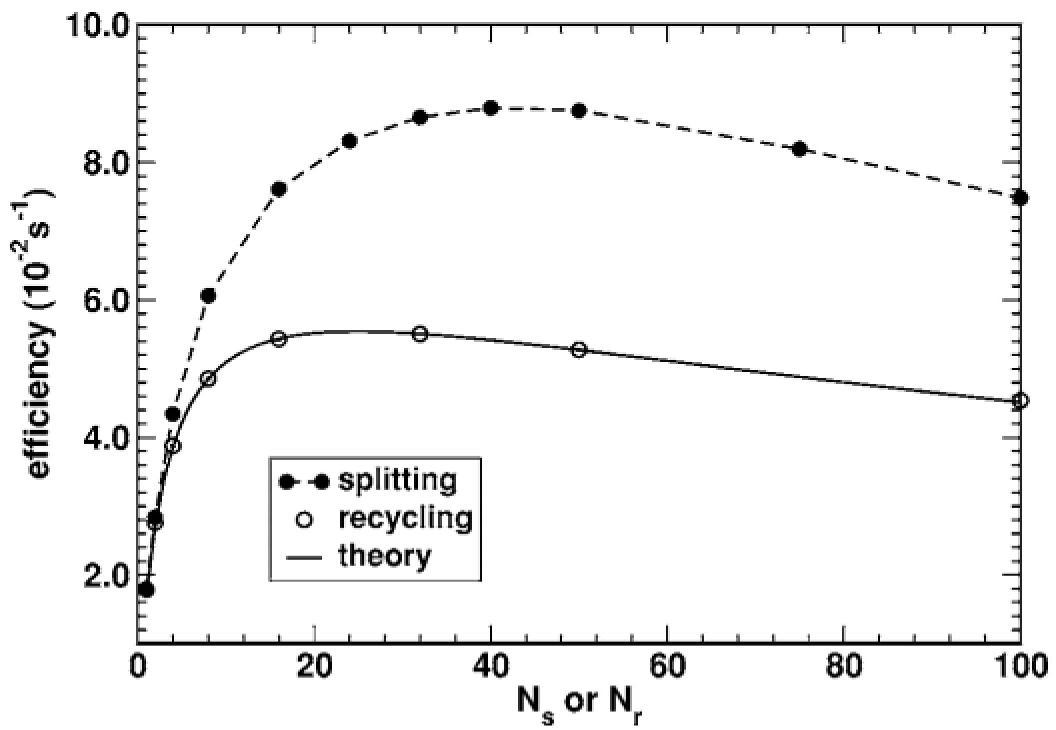

Fig. 18: increased efficiency gain comparing recycled phase space files to the DBS method implementing the splitting of photons aimed at the field of interest.

IV Examples: Research applications
IV.1 Medical linear accelerator simulations

- Technical details provided by linac manufacturers

- Models warrant experimental validation

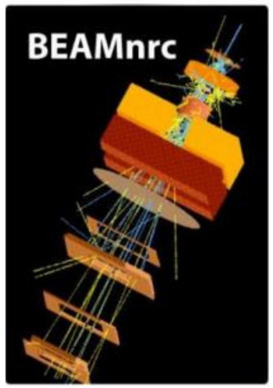

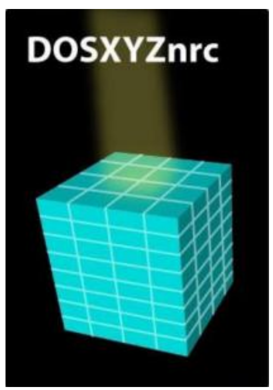

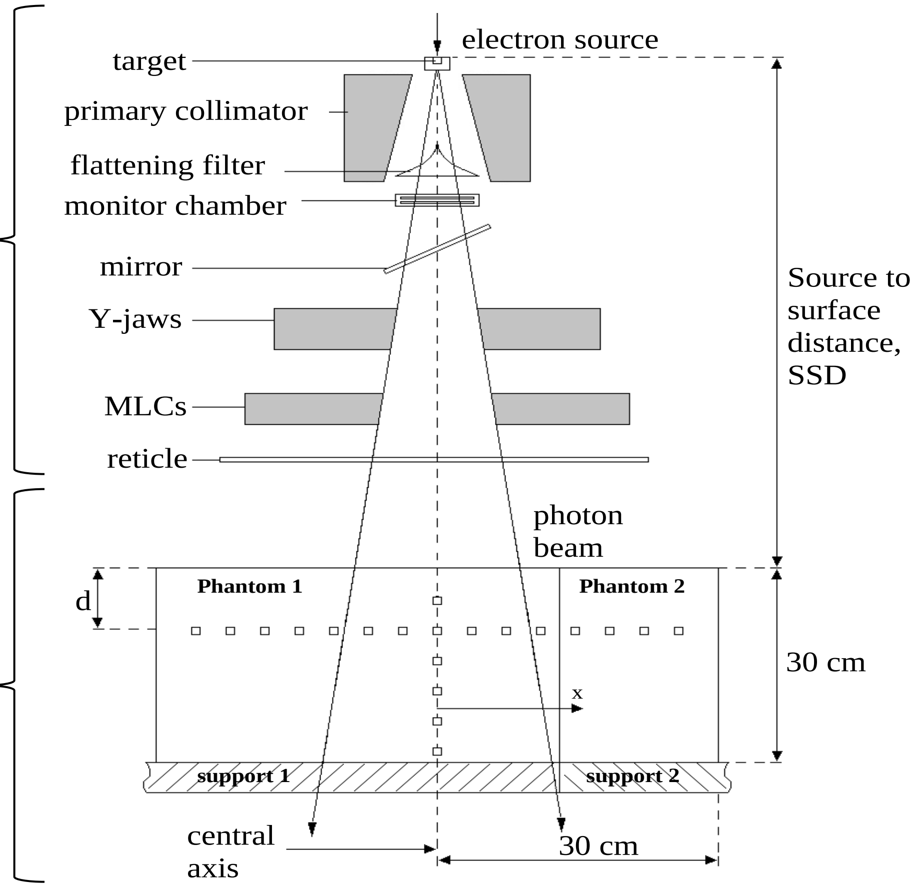

Fig. 19: Setup used for measurement or simulation of dose or spectra. Phantom 2 is removable, for investigating phantom scatter contribution.

IV Examples: Research applications
IV.1 Medical linear accelerator simulations

Lateral dose profiles

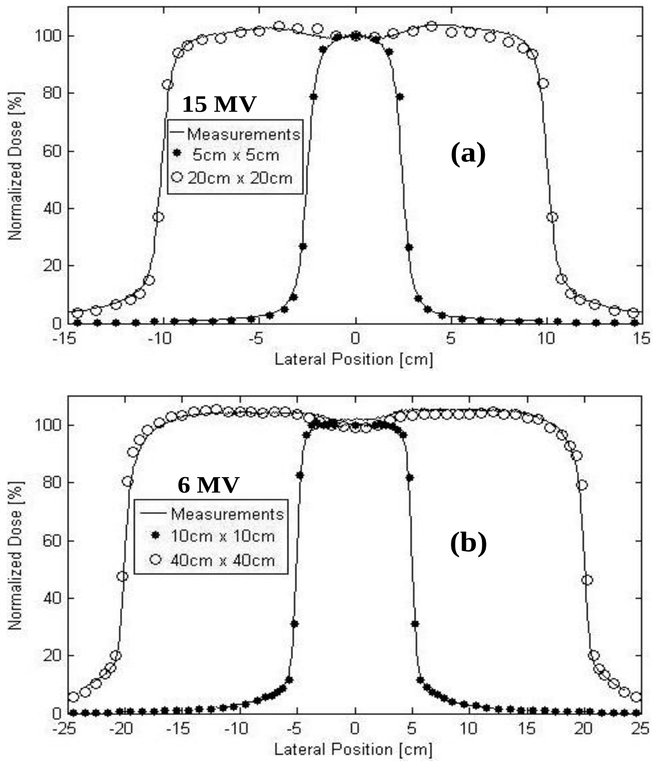

Fig. 20: Monte Carlo calculated and measured lateral dose profiles for (a) 15 MV and (b) 6 MV at SSD 90 cm and10 cm water depth.

Percent depth dose profiles

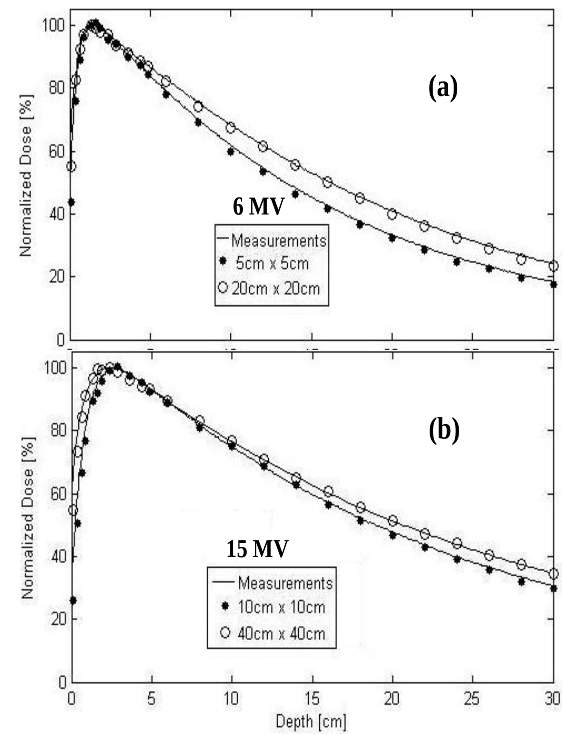

Fig. 21: Monte Carlo calculated and measured relative depth dose profiles for (a) 15 MV and (b) 6 MV at SSD 90 cm and10 cm water depth.

Table 1: Derived optimal parameters for beam-head models

Nominal photon energy, MV	Primary electron energy, MeV	FWHM of primary electron beam, mm
6	5.75	2
15	12.25	1

IV.2 Optimization of linac designs

Motivations: (i) intermediate solution between classical flattening filter and flattening filter free systems
(ii) reduction of beam-head photon and neutron leakage

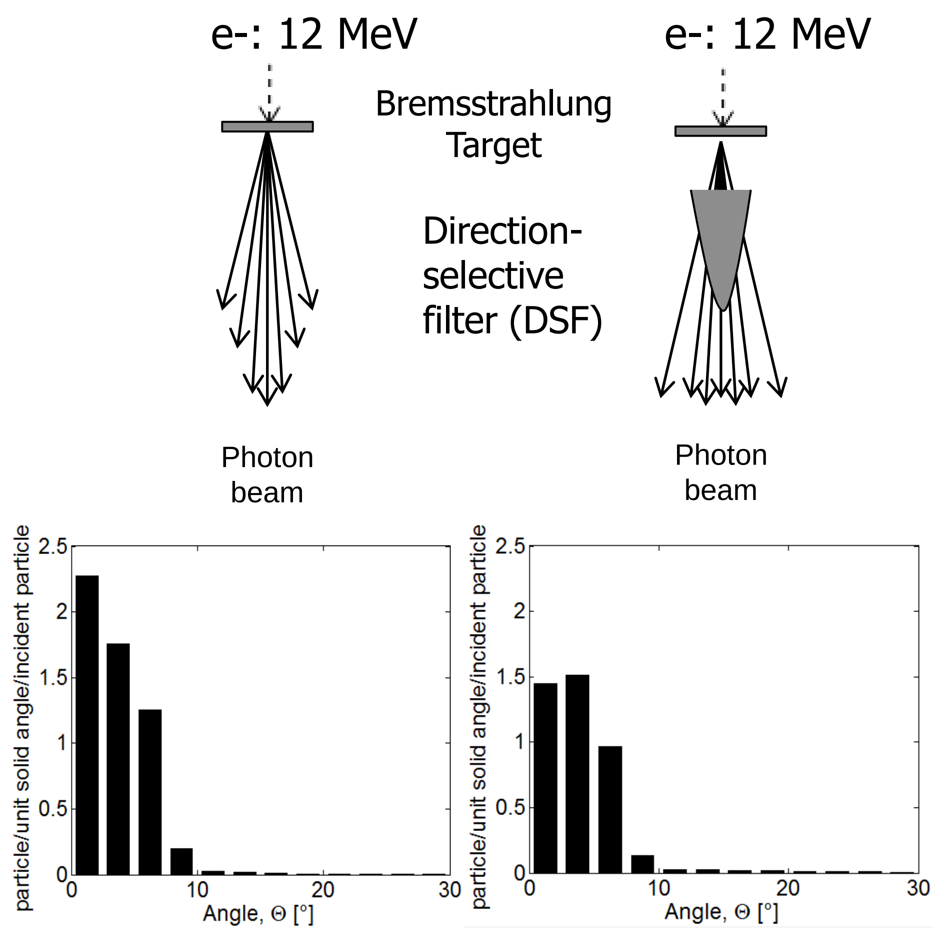

Fig. 22: Phase-space description of direction-selective filtering by small, cone-shaped filter

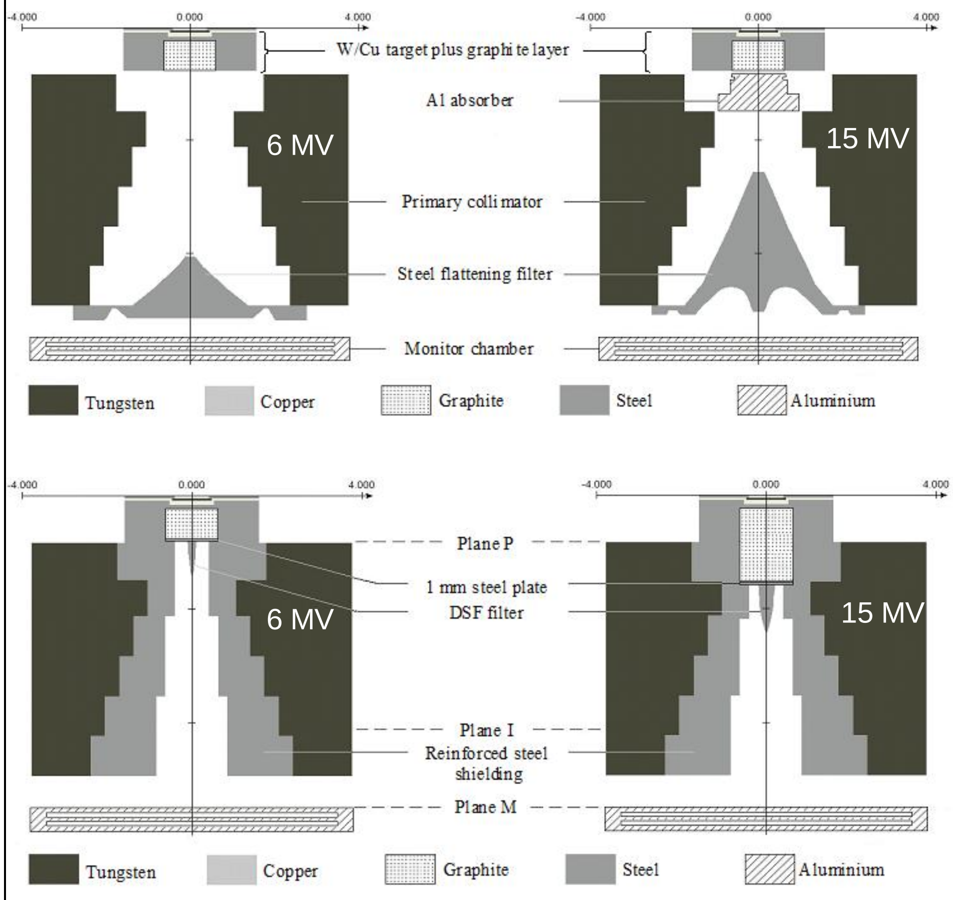

Fig. 23: Comparison of the classical flattening filter (top) with the direction-selective filter (DSF).

Photon spectra

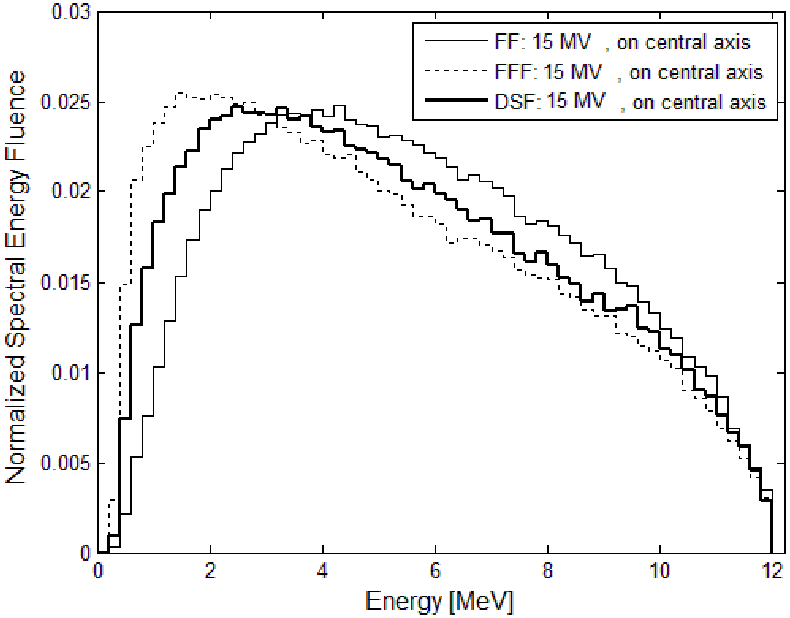

Fig. 24: Normalized values of the spectral energy fluence of 6 MV photons (a) and 15 MV photons (b) on the central axis at SSD 90 cm in air, for the beam head setups FF, FFF and DSF. The bin width is 200 keV.

Depth dose profiles

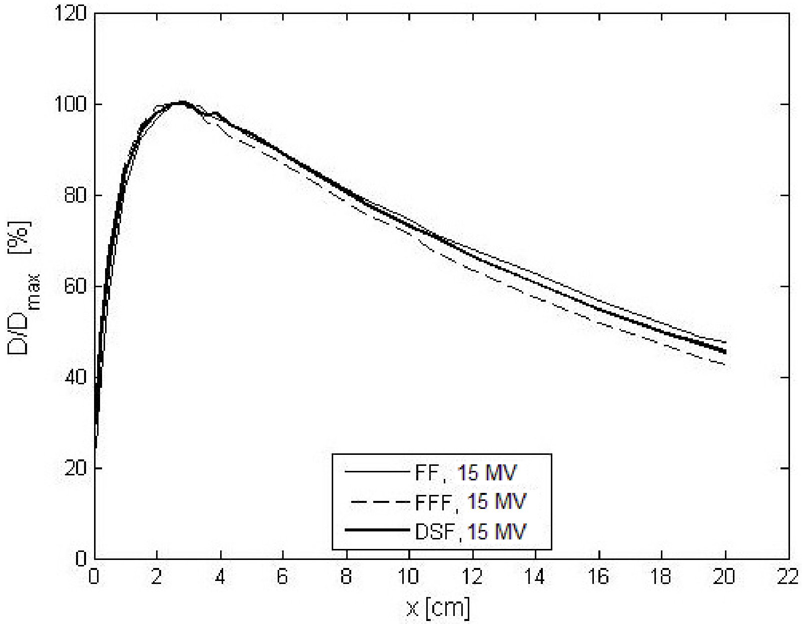

Fig. 25: Comparison of central axis percent depth-dose curves in water for 6 MV and 15 MV photons, obtained for the FF, FFF and DSF beam head setups at SSD 90 cm and for 10 x 10 cm^2 field size at 100 cm focal distance.

IV.3 Evaluation of improved shielding techniques

Motivations: (i) Evaluate sources of peripheral dose and (ii) identify and quantify its contributing components

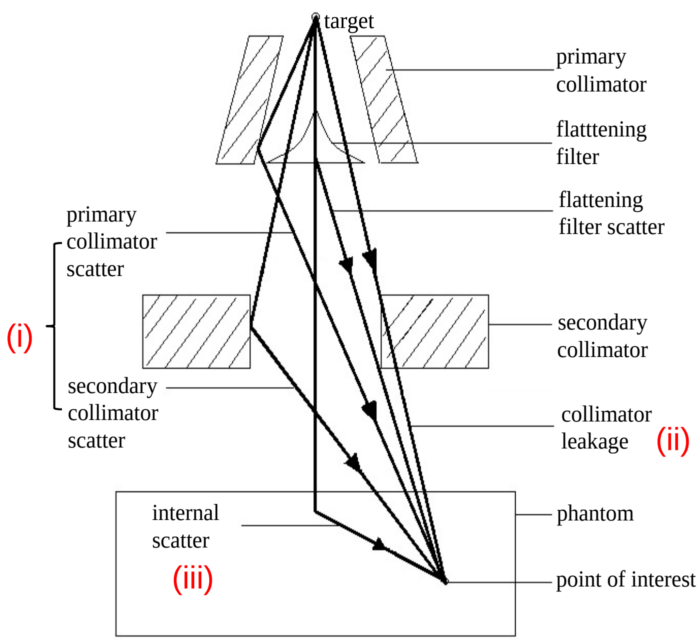

Fig. 26: Simplified display of the major components to the peripheral dose at a clinical linear accelerator. Only one of the secondary collimators is shown.

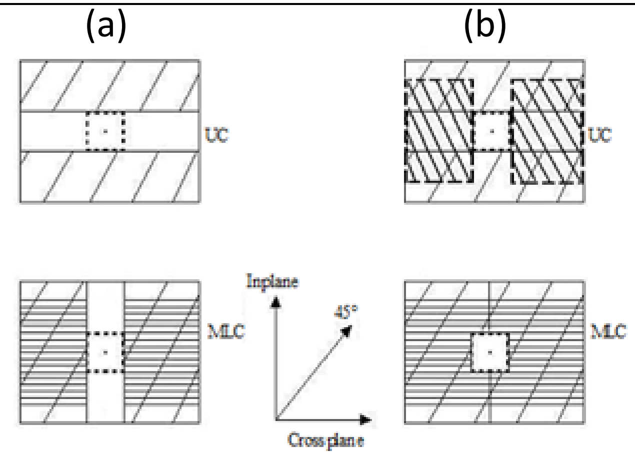

Fig. 27: Upper collimator (UC) and multileaf collimator (MLC) setup for a square field (dotted lines) (a) slits forming filed (b) optimal shielding with Y-jaws and 5 cm thick lead blocks (dotted lines), with closed MLC leaves outside field.

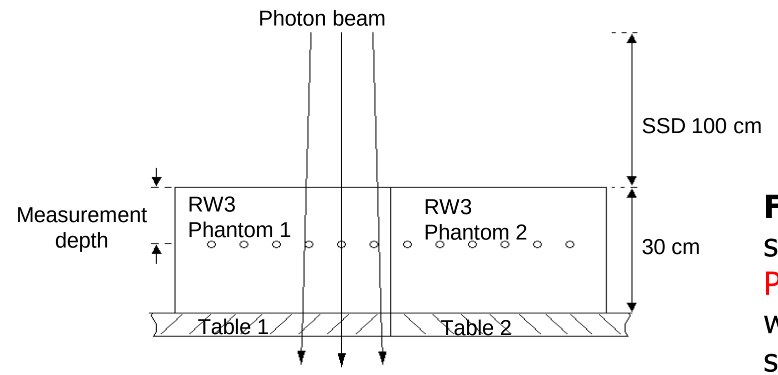

Fig. 28: Measurement setup within RW3 phantom. Phantom 1 is removable when evaluating internal scatter contributions.

Peripheral dose components:

(ii) Head transmission and leakage = No shielding – With shielding

(iii) Phantom (Internal) scatter = With phantom – No phantom

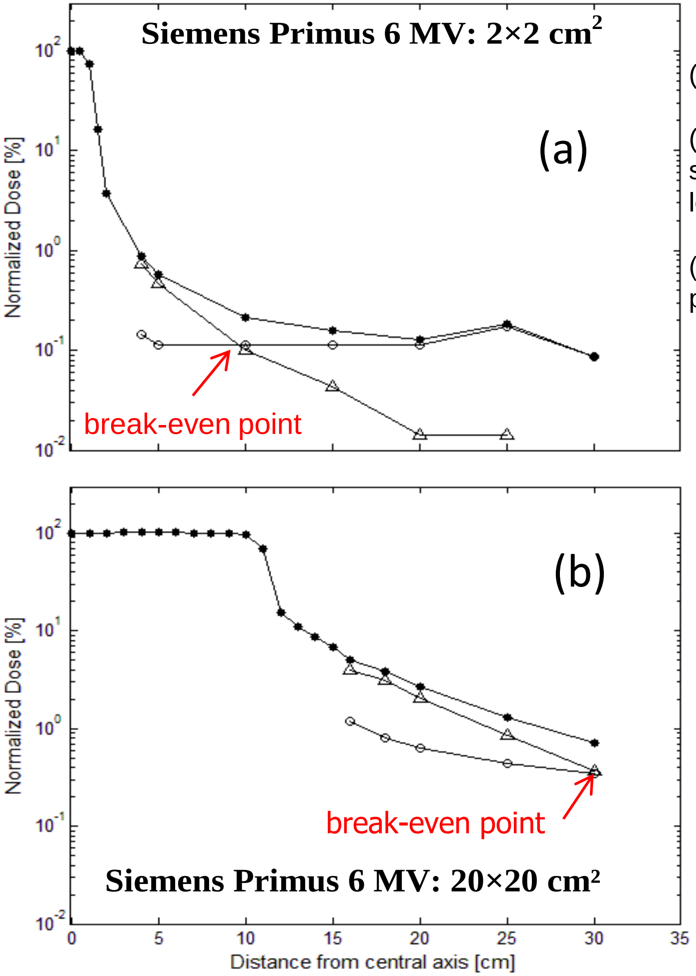

(●): total dose

(○): total dose without phantom scatter (= head scatter + head leakage)

(Δ): internal scatter dose for peripheral regions.

Fig. 29: Measured normalized dose profiles at 10 cm depth in RW3 for 2×2 cm² (a) and 20×20 cm² (b) fields, under optimal shielding conditions. Internal scatter dominates until break-even point.

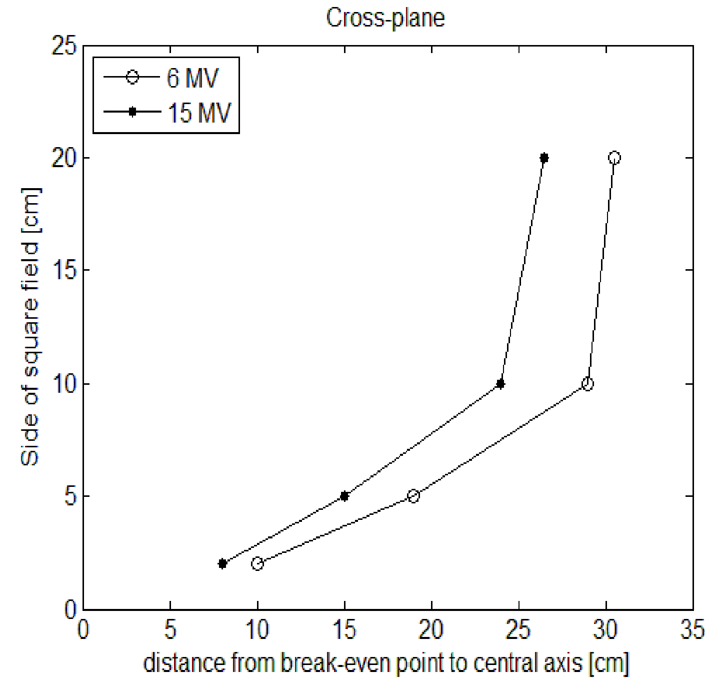

Fig. 30: Position of the break-even point for various field sizes. Characterization of the lateral extent of the contributions to peripheral dose by unavoidable (internal scatter) and avoidable (head scatter and leakage) components.

- Modelling of full detailed geometry of radiation detectors serves the purposes of:

(i) Determining correction factors due to introduction of probes within beam

(ii) Improve our knowledge of physical effects around clinical beams

(iii) Provide recommendations for clinical users (e.g. in DIN norms)

(iv) Help design optimized detectors

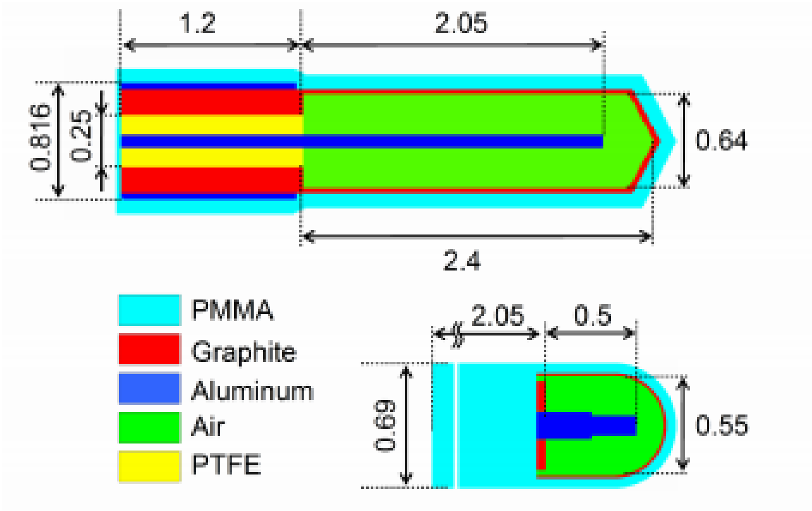

Fig. 31 cross section through models of typical thimble chambers: NE2571 Farmer chamber (top) with a sensitive air volume of 0.6 cm^3 and PTW31010 'semi-flex' (bottom) with 0.125 cm^3. The air volume is surrounded by the chamber wall and stem construction. PMMA is poly-methyl-methacrylate and PTFE is teflon. Dimensions are given in cm.

- All detector-introduced perturbation effects should be accounted for in order to trace dose measurements to primary standards

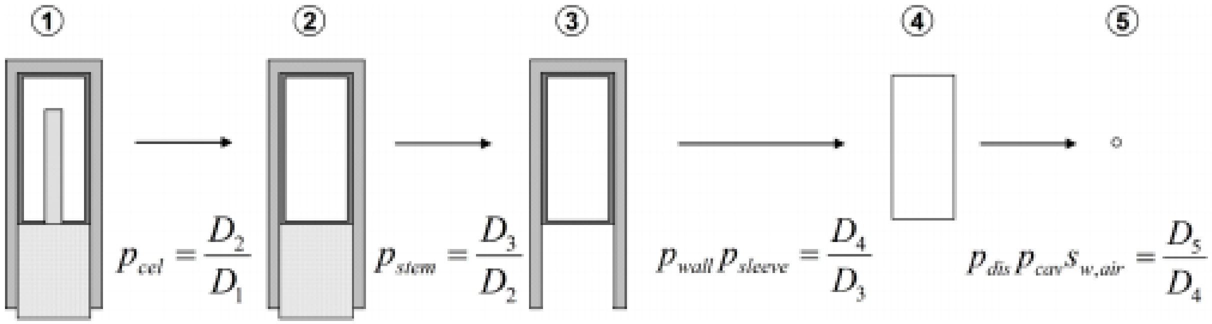

Fig. 32 Principle chain for the determination of perturbation correction factors used in this study. The various perturbation correction factors are given by the dose ratios from one step to another in the ionization chambers cavity (1-4) and the dose to a small portion of water (5). The step from model 3 to 4 can be further subdivided into separate calculation of p_{wall} and p_{sleeve}.

EGSnrc-based GMctdospp: calculation of radiation dose during computer tomography (CT) examinations

Fig. 33 Screenshot of the *GMctdospp* gui with a calculated, colored dose distribution.

IV Examples: Research applications
IV.6 Brachytherapy

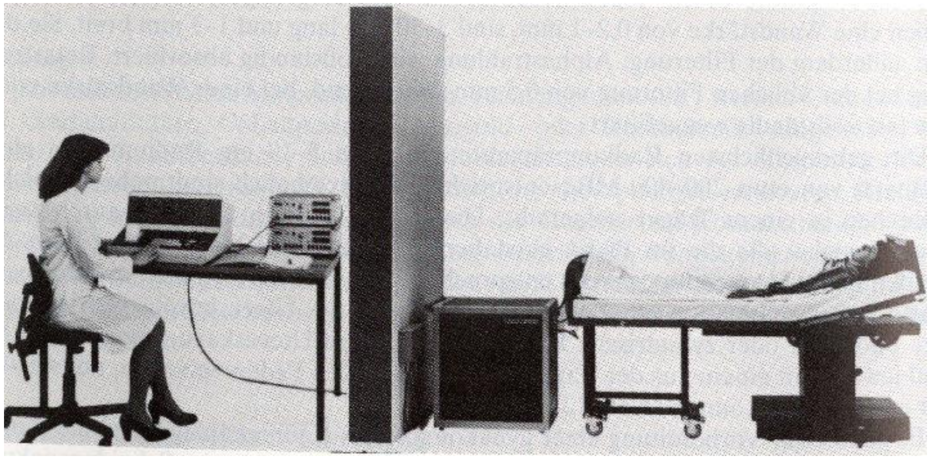

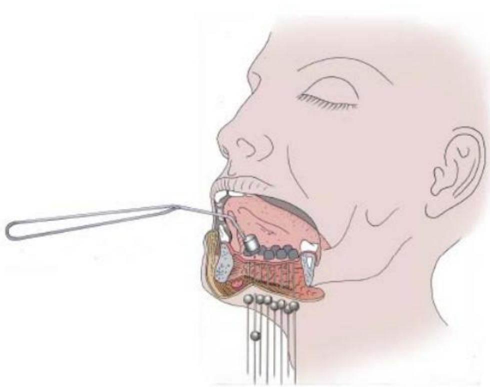

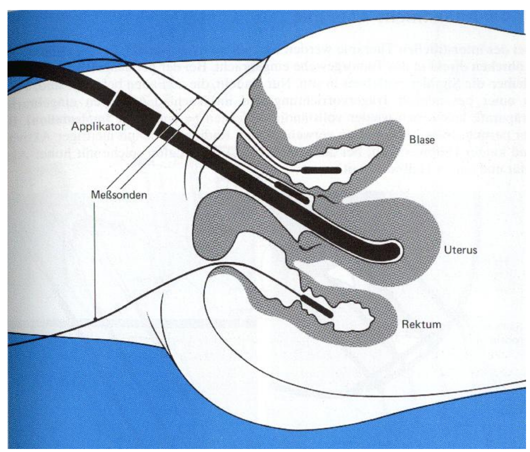

- „Tele“-therapy: radiation source outside body
- Brachy -> Greek, meaning near
- Either HDR(high dose rate, with short treatment fractions) or LDR(low dose rate, with implanted seeds over long period)
- MC for determining parameters for treatment planning systems
- Dedicated planning systems also developed for real computer tomography (CT) planning

Fig. 34: Top: typical scenario during afterloading treatment, showing the shielding wall for radiation protection purposes. Bottom: typical brachytherapy applications, such as the use of multiple sources (left) or a single source (right), with monitoring of dose to organs at risk.

- Modelling of realistic sources using DOSRZnrc cylindrical symmetric code, with up to 0.1% agreement in air kerma strengths between own simulations and literature

- 5 keV cut-off energy for photons

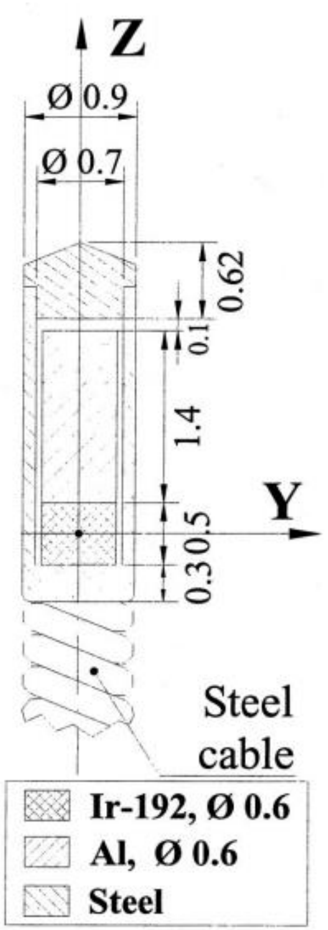

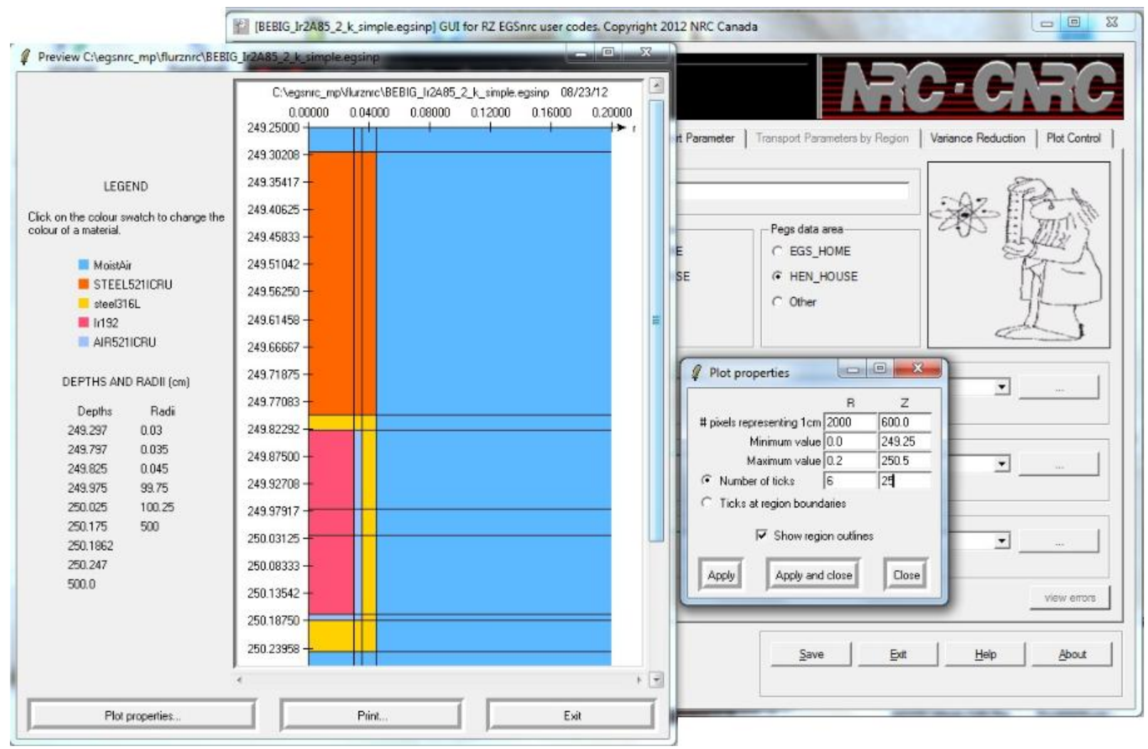

Fig. 35: Left: model of a typical high dose rate (HDR) brachytherapy source, showing dimensions in mm (not to scale). Right: Modeling of the source geometry within DOSRZnrc.

BEAMnrc

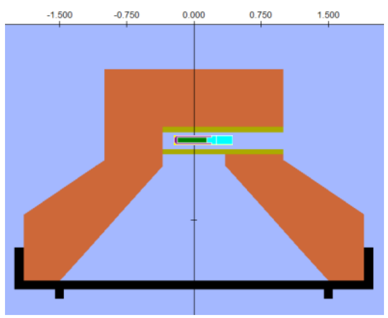

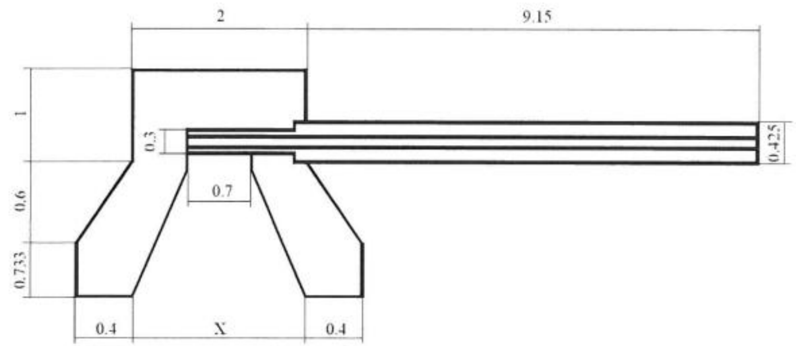

DOSXYZnrc

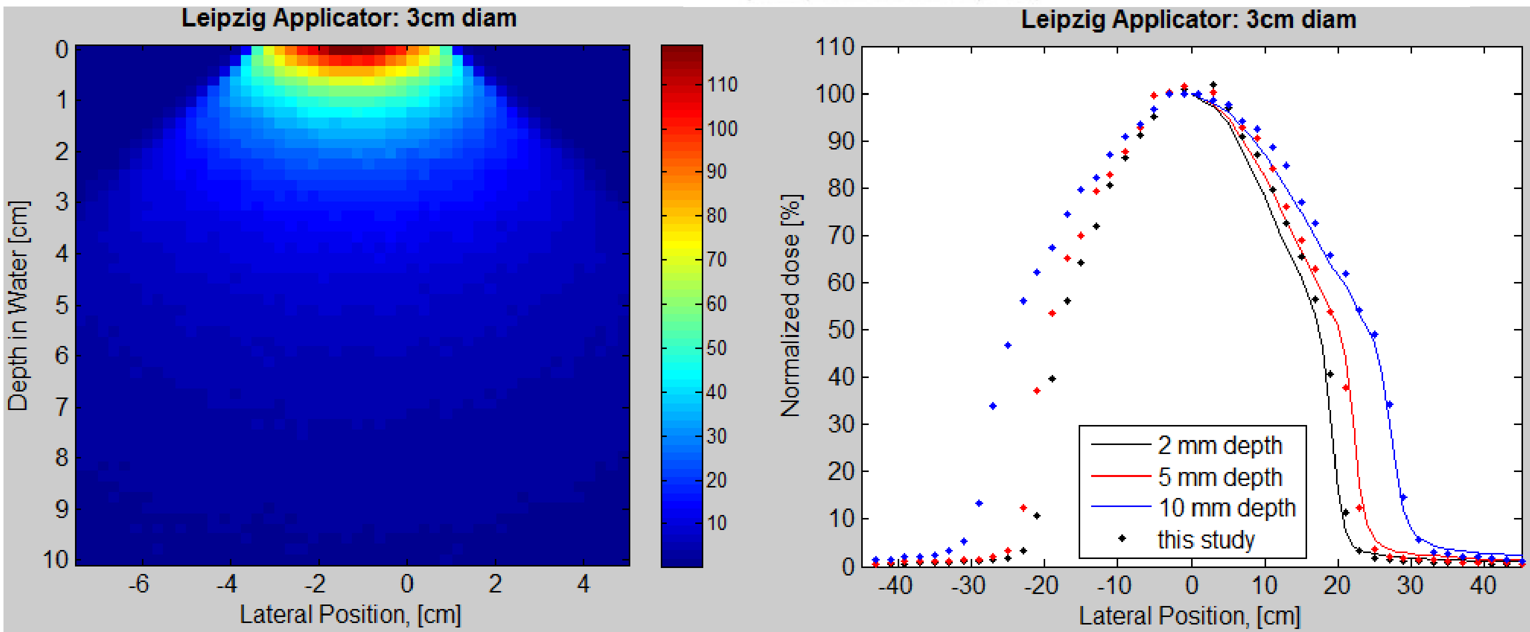

Fig. 36 Top: skin applicator design for melanoma cancer treatment. Configuration using input data from manufacturer. Bottom: Resulting dose distribution within a water phantom (left) and comparison of own simulations against published data from Niu *et al. Med Phys* 2004 (rigth).

V Commercialized MC based treatment planing systems

NOMOS: PEREGRINE

- Uses adaptive variance reduction techniques to reduce calculation time

ONCENTRA MASTERPLAN: VMC++

- Voxel Monte Carlo (VMC) code 50 to 100 times faster than EGSnrc

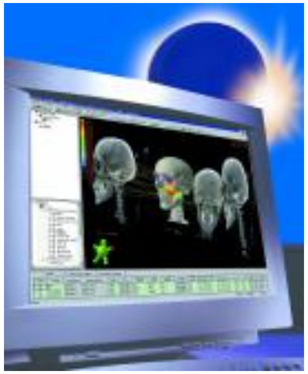

ECLIPSE: eMC (MMC)

- Derivative of voxel codes, but uses spheres to reduce storage space

Thank You

References

1. Bielajew AF. Fundamentals of the Monte Carlo method for neutral and charged particle transport. The University of Michigan. Ann Arbor. 2001
2. Calatayud JP et al. Dosimetry characteristics of the Plus and 12i Gammamed PDR Ir-192 sources. 2001 Med.Phys. 28;12: 2576-2585
3. Chofor N. The physical components of radiotherapy photon beams – a Monte Carlo and experimental study. PHD thesis. Carl von Ossietzky Universität Oldenburg
4. Kawrakow I and Walters BRB. Efficient photon beam dose calculations using DOSXYZnrc with BEAMnrc. 2006 Med.Phys. 33;8: 3046-3056
5. Niu et al. Dosimetric characteristics of the Leipzig surface applicators used in the high dose rate brachy radiotherapy. 2004 Med.Phys. 31;12: 3372-3377
6. Rogers DWO. Monte Carlo techniques in radiotherapy. 2002 Med. Phys. special issue 52;2: 63-70
7. Salvat F. Transport and interaction of electromagnetic interaction. CERN 2006
8. Schmidt R and Wulff J. Gmctdospp. http://www.thm.de/imps/programme/95-gmctdospp
9. Tessier F. Monte Carlo simulations at IRS: the EGSnrc code system. Ionising Radiation Standard. Institute of National Measurement Standards. National Research Council Canada. Workshop 2011. Ottawa.
10. Wulff J. Clinical dosimetry in photon radiotherapy- a Monte Carlo based investigation. PHD thesis. Philipps-Universität Marburg. 2010
11. Popple et al. Monte Carlo treatment planning: Implementation of clinical systems.